Plant Physiology Preview. Published on August 17, 2016, as DOI:10.1104/pp.16.00660

Reactive oxygen species tune root tropic responses

Gat Krieger[1†], Doron Shkolnik[1†], Gad Miller[2] and Hillel Fromm[1]*

[1] Department of Molecular Biology & Ecology of Plants, Faculty of Life Sciences, Tel Aviv University, Tel Aviv 69978, Israel (G.K., D.S. and H.F.), [2] Mina and Everard Goodman Faculty of Life Sciences, Bar-Ilan University, Ramat-Gan 5290002, Israel (G.M.)

Author contribution: G.K. and D.S. designed and performed experiments, analyzed the data and wrote the manuscript. H.F. and G.M supervised experiments and participated in writing the manuscript.

Funding: This research was supported by the I-CORE Program of the Planning and Budgeting Committee and The Israel Science Foundation (grant No 757/12).

Summary: Biochemical, genetic and cellular evidence shows that ROS accelerates gravitropism but attenuates hydrotropism of Arabidopsis roots

[†]These authors (in alphabetical order) equally contributed to this manuscript.

*Corresponding author's email: Hillelf@post.tau.ac.il

Abstract

The default growth pattern of primary roots of land plants is directed by gravity. However, roots possess the ability to sense and respond directionally to other chemical and physical stimuli, separately and in combination. Therefore, these root tropic responses must be antagonistic to gravitropism. The role of reactive oxygen species (ROS) in gravitropism of maize and Arabidopsis roots has been previously described. However, which cellular signals underlie the integration of the different environmental stimuli, which lead to an appropriate root tropic response, is currently unknown. In gravity-responding roots, we observed, by applying the ROS-sensitive fluorescent dye Dihydrorhodamine-123 and confocal microscopy, a transient asymmetric ROS distribution, higher at the concave side of the root. The asymmetry, detected at the distal elongation zone (DEZ), was built in the first two hours of the gravitropic response and dissipated after another two hours. In contrast, hydrotropically-responding roots show no transient asymmetric distribution of ROS. Decreasing ROS levels by applying the antioxidant ascorbate, or the ROS-generation inhibitor Diphenylene iodonium (DPI) attenuated gravitropism while enhancing hydrotropism. Arabidopsis mutants deficient in Ascorbate Peroxidase 1 (APX1) showed attenuated hydrotropic root bending. Mutants of the root-expressed NADPH oxidase RBOH C, but not *rbohD*, showed enhanced hydrotropism and less ROS in their roots apices (tested in tissue extracts with Amplex Red). Finally, hydrostimulation prior to gravistimulation attenuated the gravistimulated asymmetric ROS and auxin signals that are required for gravity-directed curvature. We suggest that ROS, presumably H_2O_2, function in tuning root tropic responses by promoting gravitropism and negatively regulating hydrotropism.

Introduction

Plants evolved the ability to sense and respond to various environmental stimuli in an integrated fashion. Due to their sessile nature, they respond to directional stimuli such as light, gravity, touch and moisture by directional organ growth (curvature), a phenomenon termed tropism. Experiments on coleoptiles conducted by Darwin in the 1880s revealed that in phototropism, the light stimulus is perceived by the tip, from which a signal is transmitted to the growing part (Darwin and Darwin, 1880). Darwin postulated that in a similar manner, the root tip perceives stimuli from the environment, including gravity and moisture, processes them and directs the growth movement, acting like "the brain of one of the lower animals" (Darwin and Darwin, 1880). The transmitted signal in phototropism and gravitropism was later found to be a phytohormone, and its redistribution on opposite sides of the root or shoot was hypothesized to promote differential growth and bending of the organ (Went, 1926; Cholodny, 1927). Over the years, the phytohormone was characterized as indole-3-acetic acid (IAA, auxin) (Kögl et al., 1934; Thimann, 1935) and the 'Cholodny-Went' theory was demonstrated for gravitropism and phototropism (Rashotte et al., 2000; Friml et al., 2002). In addition to auxin, second messengers such as Ca^{2+}, pH oscillations, Reactive Oxygen Species (ROS) and abscisic acid (ABA) were shown to play an essential role in gravitropism (Young and Evans, 1994; Fasano et al., 2001; Joo et al., 2001; Ponce et al., 2008). Auxin was shown to induce ROS accumulation during root gravitropism, where the gravitropic bending is ROS-dependent (Joo et al., 2001; Peer et al., 2013).

ROS such as superoxide and hydrogen peroxide were initially considered toxic byproducts of aerobic respiration, but currently are known also for their essential role in myriad cellular and physiological processes in animals and plants (Mittler et al., 2011). ROS and antioxidants are essential components of plant cell growth (Foreman et al., 2003), cell cycle control and shoot apical meristem maintenance (Schippers et al., 2016) and play a crucial role in protein modification and cellular redox homeostasis (Foyer and Noctor, 2005). ROS function as signal molecules by mediating both biotic- (Sagi and Fluhr, 2006; Miller et al., 2009) and abiotic- (Kwak et al., 2003; Sharma and Dietz, 2009) stress responses. Joo et al. (2001) reported a transient increase in intracellular ROS concentrations early in the gravitropic response, at the concave side of maize roots, where auxin concentrations are higher. Indeed, this asymmetric ROS distribution is required for gravitropic bending, since maize roots treated with antioxidants,

which act as ROS scavengers, showed reduced gravitropic root bending (Joo et al., 2001). The link between auxin and ROS production was later shown to involve the activation of NADPH oxidase, a major membrane-bound ROS generator, via a phosphatidylinositol 3-kinase-dependent pathway (Brightman et al., 1988; Joo et al., 2005; Peer et al., 2013). Peer et al. (2013) suggested that in gravitropism, ROS buffer auxin signaling by oxidizing the active auxin, IAA, to the non-active and non-transported form, oxIAA.

Gravitropic-oriented growth is the default growth program of the plant, with shoots growing upwards and roots downwards. However, upon exposure to specific external stimuli, the plant overcomes its gravitropic growth program and bends towards or away from the source of the stimulus. For example, as roots respond to physical obstacles or water deficiency. The ability of roots to direct their growth towards environments of higher water potential was described by Darwin and even earlier, and was later defined as hydrotropism (Von Sachs, 1887; Jaffe et al., 1985; Eapen et al., 2005).

In Arabidopsis, wild-type (WT) seedlings respond to moisture gradients (hydrostimulation) by bending their primary roots towards higher water potential. Upon hydrostimulation, amyloplasts, the starch-containing plastids in root-cap columella cells, which function as part of the gravity sensing system, are degraded within hours and recover upon water replenishment (Takahashi et al., 2003; Ponce et al., 2008; Nakayama et al., 2012). Moreover, mutants with a reduced response to gravity (*pgm1*) and to auxin (*axr1* and *axr2*) exhibit higher responsiveness to hydrostimulation, manifested as accelerated bending compared to WT roots (Takahashi et al., 2002; Takahashi et al., 2003). Recently we have shown that hydrotropic root bending does not require auxin redistribution and is accelerated in the presence of auxin polar transport inhibitors and auxin-signaling antagonists (Shkolnik et al., 2016). These results reflect the competition, or interference, between root gravitropism and hydrotropism (Takahashi et al., 2009). However, which cellular signals participate in the integration of the different environmental stimuli that direct root tropic curvature is still poorly understood. Here we sought to assess the potential role of ROS in regulating hydrotropism and gravitropism in Arabidopsis roots.

Results

Different spatial and temporal ROS patterns occur in roots in response to hydrostimulation and gravistimulation

In order to investigate the role of ROS signals in tropic responses we first assessed the spatial distribution of ROS in Arabidopsis roots responding to gravitropic stimulation. WT Arabidopsis seedlings grown vertically on agar-based medium (Materials and Methods) were gravistimulated by a 90º rotation, and monitored for their ROS distribution by applying Dihydrorhodamine-123 (DHR), a rhodamine-based fluorescent probe mostly sensitive to H_2O_2 (Gomes et al., 2005) that is often used in monitoring intracellular, cytosolic ROS (Royall and Ischiropoulos, 1993; Crow, 1997; Douda et al., 2015). DHR staining was detected in the columella, lateral root cap, epidermal layer of elongation zone (EZ) and the vasculature, and was weaker at the meristematic zone (Fig.1). This pattern is similar to previously reported staining patterns obtained by H_2O_2-specific dyes in primary roots of Arabidopsis (Dunand et al., 2007; Tsukagoshi et al., 2010; Chen and Umeda, 2015) and of other plant species (Ivanchenko et al., 2013; Xu et al., 2015). One to two hours post gravistimulation, a ROS asymmetric distribution, higher at the concave (bottom side of the root) was apparent in the epidermal layer of the distal elongation zone (DEZ), where the bending initiates (Fig.1 A). The asymmetric ROS distribution dissipated after another two hours (Fig.1 A, D), in accordance with previous reports (Joo et al., 2001; Peer et al., 2013).

To study ROS dynamics during hydrotropic growth, WT seedlings were introduced into a moisture gradient in a closed $CaCl_2$-containing chamber (herein referred to as the $CaCl_2$ / dry chamber) as previously described (Takahashi et al., 2002; Kobayashi et al., 2007; Shkolnik et al., 2016). Under this system root bending upon hydrostimulation initiates at a region more distant from the root tip compared to root bending by gravitropism. The distances of curvature from the root tip for hydrotropism and gravitropism were 601.2 ± 18.1 μm and 365.1 ± 13.1 μm, respectively (mean ± SE), 2 h post stimulation (n=29). We therefore designated the region of gravitropic bending initiation as the distal elongation zone (DEZ) and the region of hydrotropic bending initiation as the central elongation zone (CEZ), in accordance with previous definitions (Fasano et al., 2001; Massa and Gilroy, 2003). Furthermore, during the hydrotropic response, the root tip keeps facing downwards in response to gravity, where a slight curvature is detected in the DEZ (Fig.1 B, 1, 2 and 4 hours, concave side is indicated). Interestingly, during hydrotropic growth, ROS do not form an asymmetric distribution pattern at the DEZ, in contrast to the gravity-induced ROS asymmetric distribution (Fig.1 B, D). However, asymmetric distribution of

ROS appears at the CEZ, where the hydrotropic root curvature takes place and detected ROS levels are lower (Fig.1 B, D). This unequal distribution of ROS appears, however, also in roots that were subjected to non-hydrostimulating conditions (obtained by adding distilled water to the bottom the chamber), which do not undergo hydrotropic bending (Fig.1 C). Under these experimental conditions, a higher ROS level was measured at the side of the root facing the agar medium (Fig.1 C, arrowhead). The CEZ-located asymmetric distribution is not dynamic, and is maintained throughout the first four hours of the hydrotropic response without a significant change in the ratio level between the two sides of the root (Fig.1 B, D). We suspected that this asymmetric distribution of ROS may be caused by the mechanical tension formed as the root bends around the agar bed. To further test this, we used the split-agar / sorbitol system (Materials and Methods) for assessing ROS distribution during hydrotropism. In this experimental system, no asymmetric ROS distribution could be detected in response to hydrostimulation in the DEZ or CEZ (Fig.1 E, D). Moreover, we detected no changes in the overall intensity of DHR fluorescence at the indicated time points in both hydrostimulated and gravistimulated roots (Supplemental Fig.S1). Collectively, these results depict distinct dynamics and spatial patterns of ROS distribution during gravitropic and hydrotropic responses, which may imply different roles of ROS in these tropic responses. We note that strong DHR fluorescence is detected in the root vasculature above the CEZ at all time points, similar to previous reports (Tsukagoshi et al., 2010; Chen and Umeda, 2015).

ROS tune root tropic responses

To assess the possible role of ROS in hydrotropism compared to gravitropism, we tested whether ROS scavenging molecules or ROS-generation inhibitors affect hydrotropic growth. As described previously, the antioxidant ascorbic acid (ascorbate) has an inhibitory effect on root gravitropism (Joo et al., 2001; Peer et al., 2013). Indeed, our results show gravitropic bending inhibition in the presence of 1 mM ascorbate, a concentration that we found to significantly reduce ROS level at the root tip (Supplemental Fig.S2). Root curvature in control conditions was 64.9 ± 2.6 degrees, whereas in the presence of ascorbate only 49.1 ± 5.2 degrees (mean ± SE) 8 h post gravistimulation (P=0.011, Student's t test for independent measurements), without differences in root growth rates (Supplemental Fig.S3). In contrast, application of 1 mM ascorbate accelerated hydrotropic root bending. Root curvature in the $CaCl_2$ / dry chamber was 27.2 ± 2.6 degrees in control conditions whereas in the presence of ascorbate curvature was 39.3 ± 3.5 degrees (mean ± SE) 2 h post hydrostimulation (P=0.01, Student's t test for independent

measurements), and reduced root growth rate by 29.4% (Fig.2 A, B). The same trend was apparent when 1 mM of the antioxidant N-Acetyl-Cysteine was applied (not shown).

To further study the effect of ascorbate metabolism on hydrotropism we tested mutants deficient in the most abundant cytosolic ascorbate peroxidase, Ascorbate Peroxidase 1 (APX1) (Davletova et al., 2005). *apx1-2* seedlings exhibited attenuated hydrotropic bending compared to WT. Root curvature in the $CaCl_2$ / dry chamber of WT was 72.0 ± 2.8 degrees whereas that of *apx1-2* was 55.8 ± 3.5 degrees (mean ± SE) 5 h post hydrostimulation (P=$9.6 * 10^{-4}$, Student's *t* test for independent measurements), with no differences in their growth rates (Fig.2 C, D). These results were reproduced using the split-agar / sorbitol system in which the ascorbate was supplemented to the sorbitol agar slice, allowing diffusion of the chemicals towards the root tip so that the exposure to ascorbate occurs while a water potential gradient is formed (Takahashi et al., 2002; Antoni et al., 2016) (Supplemental Fig.S4 A, B). These data strongly suggest that the reduced ability to scavenge cytosolic H_2O_2 inhibited root hydrotropic bending. Unlike ascorbate-treated seedlings, gravitropic bending was not impaired or promoted in the *apx1-2* mutant (supplemental Fig.S7).

ROS generation by NADPH oxidase has opposite effects on different root tropic responses

To further study the roles of ROS in root tropisms, we tested the effects of diphenylene iodonium (DPI), an inhibitor of NADPH oxidase and other flavin-containing enzymes (Foreman et al., 2003), on hydrotropic- and gravitropic-bending kinetics and the corresponding ROS distribution patterns in primary roots. NADPH oxidase is a plasma membrane-bound enzyme that produces superoxide ($O_2^{\bullet-}$) to the apoplast (Sagi and Fluhr, 2006). Superoxide is rapidly converted to H_2O_2, which may enter the cell passively or through aquaporins (Miller et al., 2010; Mittler et al., 2011). Application of DPI accelerated hydrotropic root bending but attenuated gravitropic root bending (Fig.3). In response to hydrostimulation, root bending was accelerated in the presence of DPI, showing 86.3 ± 2.1 degrees curvature (mean ± SE) in the $CaCl_2$ / dry chamber after only 4 h, even though root growth rate was inhibited by 65.3% (Fig.3). This result was reproduced using the split-agar / sorbitol system (Supplemental Fig.S4 A).

Fluorescent ROS staining of DPI-treated roots revealed elimination of ROS from the epidermal layer of the EZ and further along the root, where ROS at the outer layers (epidermis and cortex) seemed to drop down and the remaining ROS appeared in the vasculature and its surrounding layers (Fig.4 A, B). ROS elimination at the outer root cell layers was previously

described for hydroxyphenyl fluorescein (HPF)-staining upon DPI treatment (Dunand et al., 2007). Along with decreased fluorescence at the EZ, we detected an increase of DHR fluorescence intensity at the meristematic zone of DPI-treated roots (Fig.4). Dunand et al. (2007) used nitroblue tetrazolium (NBT) for assessing extracellular $O_2^{\bullet-}$ levels in Arabidopsis root tips, and detected a decrease in NBT intensity upon DPI treatment. Since the DHR probe is mostly sensitive to cytosolic H_2O_2 (Gomes et al., 2005), our results do not contradict previously reported results.

Gravistimulated seedlings that were pre-treated for 2 h with DPI showed less ROS accumulation and consequently no ROS asymmetric distribution in the epidermal layer of the EZ, resulting in a delayed gravitropic response (Fig.4 C). Similarly, seedlings that were hydrostimulated in the presence of DPI showed elimination of ROS from the epidermal layer at the bending region, which became more proximal to the root tip (Fig.4 D). Interestingly, the gravity-directed curvature of the root tip, which occurs during hydrotropic root bending, appeared to be attenuated in ascorbate- and DPI-treated seedlings (Fig.2 A, Fig.4 D). This finding demonstrates again the negative effect of ROS elimination on root gravitropism, also in combination with a hydrotropic response.

Hydrotropism is affected by root NADPH oxidase

To further assess the inhibitory effect of ROS generation by NADPH oxidase on root hydrotropism we tested transposon-insertion mutants of the plant NADPH oxidase - RBOH (Respiratory Burst Oxidase Homolog) gene family, which consists of 10 members in Arabidopsis. These can be divided into three classes based on their tissue-specificity: RBOH D and F are highly expressed throughout the plant, RBOH A-G and I are expressed mostly in roots, and RBOH H and J express specifically in pollen (Sagi and Fluhr, 2006). RBOH C has been intensively studied, and its activity in ROS production in trichoblasts is essential for root hair elongation and mechanosensing (Foreman et al., 2003; Monshausen et al., 2009). It is expressed in trichoblasts and in the epidermal layer of the EZ (Foreman et al., 2003), though its role in the EZ is still unclear (Monshausen et al., 2009). When hydrostimulated in the $CaCl_2$ / dry chamber or in the split-agar / sorbitol systems, *rbohC* seedlings exhibited accelerated hydrotropic bending. Measured in the $CaCl_2$ / dry chamber, root curvature in WT was 46.4 ± 3.1 degrees compared to 64.2 ± 3.5 degrees in *rbohC* (mean ± SE) 2 h post hydrostimulation (P=$5.1 * 10^{-4}$, student's *t* test for independent measurements) with no difference in growth rate compared to WT (Fig.5 A,

B; Supplemental Fig.S4 C; Supplemental movie 1). We then examined the hydrotropic response of seedlings deficient in RBOH D, which has the highest expression levels among the RBOHs. RBOH D is expressed in all plant tissues but mainly in stems and leaves and is known as a key factor in ROS systemic signaling (Sagi and Fluhr, 2006; Miller et al., 2009; Suzuki et al., 2011). Interestingly, *rbohD* seedlings did not exhibit significantly-different hydrotropic bending kinetics or root growth rates compared to WT (Fig. 5 A, B; Supplemental Fig.S4 C; Supplemental movie 2). DHR staining revealed no significant difference in ROS spatial patterns in gravistimulated nor hydrostimulated (using the $CaCl_2$ / dry chamber or split-agar / sorbitol system) roots of the RBOH mutants, compared to WT (Supplemental Fig.S5-S8). Therefore, to better characterize endogenous ROS levels in root tissues of wt and *rbohc* and *rbohd* mutants, we applied Amplex red for determination of H_2O_2 content in tissue extracts (Materials and Methods). When examining extracts from whole seedlings, we observed a 68% and 77% reduction in H_2O_2 levels in *rbohD* and *rbohC*, respectively, compared to WT (Fig.5 D). We then examined extracts from excised root apices (1-2 mm from tip) and observed a relatively similar H_2O_2 content in WT and *rbohD* roots, while *rbohC* mutants showed a 57% reduction in H_2O_2 content compared to WT (Fig.5 C). These results are consistent with the tissue-specific expression pattern of the two RBOHs, as RBOH C is highly expressed in roots, while RBOH D is not (Sagi and Fluhr, 2006) and with the accelerated hydrotropic phenotype of *rbohC* compared to *rbohD* and wt. Their different expression patterns could also be visualized in the high-resolution spatiotemporal map (Brady et al., 2007) of the eFP browser (Winter et al., 2007).

The acceleration in hydrotropic root bending of *rbohC* is however weaker compared with that of DPI-treated WT seedlings (measured in the $CaCl_2$ / dry chamber, root curvature in *rbohC* was 75.41±2.19 degrees and root curvature of DPI treated seedlings was 86.31±2.11 degrees after 4 h of hydrostimulation, while WT and DMSO-treated WT roots exhibited 63.27±2.38 and 62.67±3.17 degrees in that time, respectively). These results may indicate partial functional redundancy with other root-expressed RBOHs, or involvement of other DPI-sensitive enzymes in this tropic growth. When treated with DPI, *rbohC* roots presented the same hydrotropic bending kinetics as WT roots (not shown). Unlike DPI-treated seedlings, RBOH C- and RBOH D-deficient mutants did not show inhibition or acceleration in their gravitropic growth (Supplemental Fig.S8) nor weakened gravity-directed curvature of the root tip during hydrotropic growth (Fig.5) and gravitropic ROS asymmetric distribution as in WT (Supplemental Fig.S7). These results may be explained by functional redundancy between the

root-expressed RBOH family members, as well as by compensation of ROS signaling by mechanisms involved specifically in gravitropism.

Hydrotrostimulation attenuates the gravitropic ROS and auxin signals

In order to test a possible direct link between hydrotropism and gravitropism through ROS, we challenged WT seedlings with combined stimuli using the split-agar / sorbitol method (Fig.6 A). The split-agar system allows slow and controlled exposure of the root tips to increasing osmotic pressure, and by rotation of the chamber allows changes in the gravity vector (Fig.6 A). After 0-2 h of hydrostimulation, 1 h of gravistimulation induced a clear asymmetric ROS distribution at the bending EZ. After 3 h of hydrostimulation, 1 h of gravistimulation generated a weak asymmetric ROS distribution (Fig.6 B, C). Strikingly, following 4 h of hydrostimulation, 1 h of gravistimulation failed to generate an asymmetric ROS distribution, and gravity-directed root bending was not observed (Fig.6 B, C). These results indicate that as the osmotic stress stimulus increases and promotes hydrotropic curvature, gravistimulation is not sufficient to evoke typical ROS asymmetric distribution, and growth towards higher water potential is favorable. Indeed, with increasing hydrostimulation time from 0 to 4 hr prior to gravistimulation, gravitropic curvature decreased (Fig.6 D). Four hrs of hydrostimulation prevented gravitropic curvature as roots responded only to the hydrotropic stimulus (depicted as a negative curvature angle in Fig.6 D).

Subsequently, in order to assess whether the attenuation of the ROS signal of gravistimulated roots following hydrostimulation is associated with the attenuation of auxin distribution, roots of DII-VENUS-expressing transgenic seedlings (Brunoud et al., 2012) were gravistimulated for 1 h following exposure to an osmotic gradient for 0, 2 or 4 h (Supplemental Fig.S9). With this auxin reporter, lower levels of DII-VENUS fluorescence indicate higher levels of auxin. In agreement with the ROS signal dynamics, we observed asymmetric auxin distribution in the lower part of the root tip (concave) in roots that were gravistimulated with no prior hydrostimulation, or following 2 h of hydrostimulation (Supplemental Fig.S9), as previously demonstrated in graviresponding roots (Band et al., 2012). However, hydrostimulation for 4 h prior to gravistimulation impaired the generation of an auxin gradient across the root tip (Supplemental Fig.S9). Based on the known relationship between auxin and ROS in gravistimulation, these results may suggest that hydrotropic stimulation attenuates the

gravitropic ROS signal through the interruption of auxin distribution. However, we cannot exclude the possibility that hydrostimulation attenuates gravistimulated ROS and auxin distribution through independent signaling pathways that are yet to be elucidated.

Discussion

In order to perform hydrotropic bending, a root must overcome its gravity-directed growth (Eapen et al., 2005; Takahashi et al., 2009). Our results suggest opposite roles for ROS in hydrotropic and gravitropic growth behaviors. When treated with ascorbate, an antioxidant, or DPI, an inhibitor of NADPH oxidase and other flavin-containing enzymes (Foreman et al., 2003), Arabidopsis primary roots exhibit opposite changes in their bending kinetics in response to the different stimulations, namely, delay in gravitropism and acceleration in hydrotropism (Fig.2, 3 ,Supplemental Fig. S3 and Supplemental Fig.S4). The antagonism between these two responses was shown previously for the agravitropic pea mutant (*ageotropum*), whose lack of gravity response contributes to its hydrotropic responsiveness (Takahashi and Suge, 1991). Amyloplast degradation at early stages of a hydrotropic response may also be a mechanism by which the root eliminates its sense of gravity in order to perform non-gravitropic growth (Takahashi et al., 2003; Ponce et al., 2008). When examining the ROS and auxin patterns in response to combined stimuli by first applying hydrostimulation and afterwards applying both hydro- and gravistimulation, we observed a reduction in gravity-directed ROS-asymmetry and auxin-gradient when the duration of hydrostimulation is increased (Fig.6, Supplemental Fig.S9). We therefore conclude that during hydrotropic growth, the root actively attenuates gravitropic auxin and ROS signaling to overcome gravitropic growth.

In gravitropism, auxin is required for ROS production (Joo et al., 2005; Peer et al., 2013). In contrast, neither auxin redistribution nor auxin signaling are required for hydrotropic bending (Shkolnik et al., 2016). Moreover, inhibition of polar auxin transport or Transport Inhibitor Response (TIR)-dependent signaling accelerate hydrotropism (Shkolnik et al., 2016). Consistent with these observations, asymmetric distribution of ROS was not detected in the DEZ during hydrotropism. In gravitropism, however, both an auxin gradient at the lateral root cap, and ROS asymmetric distribution at the DEZ are formed transiently. Collectively, these results demonstrate the antagonism between hydro- and gravitropism with respect to auxin- and ROS-signaling.

Asymmetric ROS distribution was however observed in the CEZ of hydrostimulated roots in the $CaCl_2$ / dry chamber system, and its asymmetry ratio level has not changed during the measured time points (Fig.1 B, D). This asymmetric pattern, i.e., higher ROS levels at the side of the root that is in contact with the agar medium, was also present in roots that were exposed to non-hydrostimulating conditions and do not perform hydrotropic bending (Fig.1 C, D). Therefore, this non-transient unequal distribution of ROS in the CEZ may be a result of mechanosensing-induced ROS (Monshausen et al., 2009) at the region where the root detaches from the agar medium. Indeed, no ROS asymmetry was observed in roots exposed to a water-potential gradient in the split-agar / sorbitol system (Fig.1 E,D), where the root does not encounter mechanical tension by the agar due to bending. Therefore it is clear that hydrotropism does not involve asymmetric distribution of ROS. Yet, it attenuates gravity-directed asymmetric ROS distribution.

In addition to their roles as intracellular signaling molecules, ROS function in several apoplastic processes, including cell wall rigidification that is thought to restrict cell elongation (Hohl et al., 1995; Monshausen et al., 2007). It is tempting to hypothesize that in gravitropism, the higher levels of ROS in the concave side of the root promote root bending by inhibition of cell elongation at this side. However, this hypothesis fails to explain the opposite effects of antioxidants and ROS-generator inhibitors on gravi- and hydrotropism, as differential cell elongation is needed in both cases.

In this study, we show that ROS, presumably cytosolic H_2O_2 in the epidermal layer of the root EZ, negatively regulate hydrotropic bending. The activity of RBOH C was characterized as essential for this process, since *rbohC* mutants showed accelerated hydrotropic root bending and lower levels of H_2O_2 in the root apex (Fig.5). This, however, does not exclude the possible contribution of other root-expressed RBOHs or other flavin-containing enzymes to the process. The localization of ROS-generating enzymes of the RBOH family has substantial effects on the tissue-specific ROS levels and the consequent hydrotropic root curvature, as it appears that in mutants deficient in RBOH D, which is expressed throughout the plant but mostly in leaves and stems (Suzuki et al., 2011) ROS levels in the root apex and hydrotropic curvature were similar to those of WT (Fig.5, Supplemental Fig.S3). As for ROS scavenging enzymes, we detected a weak hydrotropic root bending in *apx1-2* mutants (Fig.2, Supplemental Fig.S3), which lack the function of the abundant cytosolic H_2O_2-scavenging enzyme APX1 and are thus expected to accumulate higher H_2O_2 levels in all plant tissues. Peroxidases were shown to play an important

role in root development and growth control (Dunand et al., 2007) by modifying $O_2^{\bullet-}$ to H_2O_2 at the transition-to-elongation zone (Tsukagoshi et al., 2010). Our observations are consistent with this ROS type-specific accumulation pattern, and add a new aspect to the role of H_2O_2 at the root EZ.

The phytohormone abscisic acid (ABA) was previously reported as a positive regulator of root hydrotropism. Arabidopsis mutants deficient in ABA-sensitivity (*abi2-1*) and ABA-biosynthesis (*aba1-1*) were reported as less responsive to hydrostimulation, whereas ABA treatment rescued the delayed hydrotropic phenotype of *aba1-1* (Takahashi et al., 2002). ABA-signaling involves the activation of Pyrabactin Resistance/PYR1-like (PYR/PYL) receptors that mediate the inhibition of clade A phosphatases type 2C (PP2C), which are negative regulators of the pathway (Antoni et al., 2013). The involvement of this pathway in root hydrotropism was demonstrated recently, as a *pp2c*-quadruple mutant exhibited an ABA-hypersensitive phenotype and consequently enhanced hydrotropic response, while a mutant deficient in six PYR/PYL receptors exhibited insensitivity to ABA treatment and to hydrotropic stimulation (Antoni et al., 2013). Since ABA was shown to induce stomata closure through the activation of the NADPH oxidases RBOH D and RBOH F (Kwak et al., 2003), it is tempting to hypothesize that ABA activates ROS production in root-expressed NADPH oxidases during hydrotropic growth. A candidate mediator for this process may be PYL8, since PYL8-deficient mutants (*pyl8-1* and *pyl8-2*) exhibited a non-redundant ABA-insensitive root growth when treated with ABA, and transcriptional fusion of PYL8 (*ProPYL8:GUS*) revealed its expression in the stele, columella, lateral root cap and root epidermis cells (Antoni et al., 2013). The latter expression region overlaps with that of RBOH C (Foreman et al., 2003). However, distinguished from their role in stomata closure, ROS negatively regulate hydrotropism and thus may function in a negative feedback to ABA signaling. Antagonism between ROS and ABA also appears in seed germination, as H_2O_2 breaks ABA-induced seed dormancy in several plant species (Sarath et al., 2007).

In the context of integration of environmental stimuli by the root tip (Darwin and Darwin, 1880), we suggest that ROS, presumably cytosolic hydrogen peroxide, fine tune root tropic responses by acting as positive regulators of gravitropism and as negative regulators of hydrotropism. Root hydrotropism and gravitropism differ in several aspects, such as the time of response (Eapen et al., 2005), the region of bending initiation (reported in this study), the involvement of auxin (Kaneyasu et al., 2007; Shkolnik et al., 2016) and the effect of ROS on the

response kinetics. In order to elucidate the effects of ROS on tropic responses, their downstream effectors in gravitropism and hydrotropism need to be characterized.

Materials and Methods

Plant material and growth conditions

Wild type Arabidopsis thaliana (Col-0) and T-DNA/Transposon insertion mutants: *rbohC* (*rhd2*), *rbohD* (Miller et al., 2009) and *apx1-2* (SALK_000249) (Suzuki et al., 2013) were used in this research. For vapor sterilization, seeds were put inside a desiccator next to a glass beaker containing 25 ml water, 75 ml bleach and 5 ml HCl for 2 h. Sterilized seeds were sown on 12 x 12 cm squared Petri dishes, containing 2.2 gr/L Nitsch & Nitsch medium (Duchefa Biochemie B.V., Haarlem, the Netherlands) titrated to pH 5.8, 0.5 % (w/v) sucrose supplemented with 1 % (w/v) plant agar (Duchefa) and vernalized for one day in 4º C in dark. Plates were put vertically in a growth chamber at 22º C and day light (100 µE m^{-2} sec^{-1}) under 16/8 light/dark photoperiod. The root hair-deficient phenotype of *rbohC* was observed when grown on pH 5-titrated growth medium. Treatments with 10 µM DPI (Diphenyleneiodonium chloride, Sigma) dissolved in Dimethyl Sulfoxide (DMSO), 1 mM Sodium Ascorbate (Sigma) dissolved in distilled water and 1 mM N-acetyl-cysteine (Acros organics) dissolved in distilled water were performed by applying these chemicals in the agar medium. Ascorbate treatment for DHR staining was performed by transferring seedlings onto 1 mm Whatman filter paper 0.25 X Murashige and Skoog medium (MS) (Murashige and Skoog, 1962) and the indicated ascorbate concentrations.

Hydrotropic stimulation assays

A $CaCl_2$ dry chamber was designed based on a previously described system (Takahashi et al., 2002; Kobayashi et al., 2007; Shkolnik et al., 2016) with the following modifications: Plates were prepared as described in 'Plant material and growth conditions' with or without supplemented chemicals, as indicated. The medium was cut 6 cm from the bottom and 5-7 day-old seedlings were transferred to the cut medium, such that approximately 0.2 mm of the primary root tip was bolting from the agar into air. Twelve ml of 40 % $CaCl_2$ (w/v) (Duchefa) were put at the bottom of the plate, which was then closed, sealed with Parafilm and placed vertically under 30 µE m^{-2} sec^{-1} white light. As control, non-hydrostimulating conditions were achieved by adding 20 ml of distilled water to the bottom of the plate. In this system, the roots were exposed to the supplemented chemical at the beginning of the experiment. Hydrostimulation was performed also using the previously described split-agar method (Takahashi et al., 2002; Antoni

et al., 2016). Ascorbate, DPI or DMSO (control) were added directly to the sorbitol containing gel slice. Root tips were imaged at indicated time points using Nikon D7100 camera equipped with AF-S DX Micro NIKKOR 85 mm f/3.5G ED VR lens (Nikon, Tokyo, Japan). For root curvature measurements and supplemental movies of the humidity-gradient system, plates were faced ~45 º to the lens, and multiple photos with changing focus were obtained using Helicon remote software, and stacked using Helicon focus software (www.heliconsoft.com). Root curvature and growth were analyzed using ImageJ software 1.48V (Wayne Rasband, NIH, USA).

Gravitropic stimulation assay

Five to seven-day-old seedlings were transferred to a standard medium, or ascorbate containing medium, following one hour of acclimation at original growth orientation before the plates were 90º rotated. For DPI treatment, seedlings were pre-treated in DMSO or 10 µM DPI-containing media for 2 h, then transferred to another plate containing standard medium, followed by 30 min acclimation at the original growth orientation before the plates were rotated by 90º.

Confocal microscopy

For ROS detection, seedlings were immersed in 86.5 µM [0.003% (w/v)] Dihydrorhodamine-123 (Sigma) dissolved in Phosphate Buffer Saline (PBS x 1, pH 7.4) for 2 or 5 min, after hydrotropic or gravitropic stimulation assays. Fluorescent signals in roots were imaged with a Zeiss LSM 780 laser spectral scanning confocal microscope (Zeiss, http://corporate.zeiss.com), with a 10X air (EC Plan-Neofluar 10x/0.30 M27) objective. Acquisition parameters were as follows: master gain was always set between 670 and 720, with a digital gain of 1, excitation at 488 nm (2%) and emission at 519-560 nm. Signal intensity was quantified as mean grey value using ImageJ software. Confocal images were pseudo-colored using the RGB look-up table of the ZEN software, for easier detection of the fluorescent signal distribution in the root. Imaging of DII-VENUS expressing roots was performed as previously described (Shkolnik et al., 2016).

Determination of H_2O_2 in tissue extracts

Whole seedlings (n = 20 seedlings) and root apices (1-2 mm from root tip, n = 60 seedlings) were frozen in liquid nitrogen and homogenized in Phosphate Buffer Saline (PBS x 1, pH 7.4) (600 µl for whole seedlings and 150 µl for root apices), centrifuged in 10,000 g for 5 min in 4° C and the supernatant was used as the tissue extract. H_2O_2 levels in the extracts were measured using the Amplex red assay kit (Molecular Probes, Invitrogen) according to the manufacturer's protocol, with 3 biological repeats and two technical replicates. Samples were measured with a

Synergy HT fluorescence plate reader (BioTek) using 530/590 nm excitation/emission filters. Protein levels in the extracts were determined using the Bradford reagent (Bio-Rad). The absorbance was read in the same plate reader using a 595 nm filter. Fluorescence reads were then normalized to the protein amount.

Statistical analysis

Results were analyzed using MS Excel ToolPak and R version 3.1.1.

Supplemental materials

Figure S1: Relative DHR fluorescence intensity in gravistimulated and hydrostimulated roots.

Figure S2: ROS level is reduced by ascorbate.

Figure S3: The antioxidant ascorbate impedes root gravitropic response.

Figure S4: Hydrostimulation using the split-agar / sorbitol method.

Figure S5: ROS distribution during hydrotropic growth in WT, *rbohC* and *rbohD* mutants.

Figure S6: ROS distribution in hydrostimulated WT, *rbohC* and *rbohD* mutants using the split-agar / sorbitol system.

Figure S7: ROS distribution in gravistimulated WT, *apx1-2*, *rbhoC* and *rbhoD* mutants.

Figure S8: *rbohC* and *rbohD* exhibit normal gravitropic growth compared to WT.

Figure S9: Auxin distribution in gravistimulated root tips with or without prior hydrostimulation.

Video movie-1: Hydrotropism of *rbohC* mutant compared to wt.

Video Movie-2: Hydrotropism of *rbohD* mutant compared to wt.

Acknowledgements

This research was supported by the I-CORE Program of the Planning and Budgeting Committee and The Israel Science Foundation (grant No 757/12). We thank Professor Robert Fluhr for

critical reading of the manuscript, and lab members Yosef Fichman and Roye Nuriel for helpful suggestions.

Figure Legends

Figure 1: ROS spatial and temporal distribution patterns during root gravitropism and hydrotropism. A, B, C and E) Confocal microscopy of 5-day old seedlings stained with Dihydrorhodamin-123 (DHR), a ROS-sensitive fluorescent dye. Images were pseudo-colored, red indicates higher ROS-dependent fluorescence intensity. Scale bars, 100 μm. DEZ, Distal Elongation Zone, CEZ, Central Elongation Zone (designated according to Fasano et al., 2001). White lines next to the root mark defined root zones. g represents gravity vector, Ψ represents water potential gradient. Concave and convex sides of the root are indicated. Arrowheads point to regions where the fluorescence signal distributes unevenly between the two sides of the root. A) Under gravistimulation, an asymmetric distribution of ROS was apparent 2 h post stimulation and dissipated after another 2 h. This asymmetry was detected at the DEZ where higher ROS levels were observed at the concave side of the root. B) Under hydrostimulation, ROS distribute asymmetrically at the CEZ however maintain symmetric distribution at the DEZ. C) The asymmetric ROS pattern at the CEZ was also observed in roots that were exposed to non-hydrostimulating conditions and do not bend hydrotropically. The higher ROS level was observed at the side that is in contact with the agar medium. D) Quantification of DHR fluorescence, measured at the epidermal layer in two regions of the root EZ (in the DEZ of gravistimulated roots and in the DEZ and CEZ of hydrostimulated roots). The data is presented as the ratio between the signal at the concave and the convex sides of the root. Error bars represent mean ± SE (3 biological independent experiments, $14<n<23$). **$p < 0.01$, Student's t-test versus start time. E) Roots were hydrostimulated for the indicated times using the split-agar / sorbitol system. F) Quantification of DHR fluorescence, measured at the DEZ epidermal layer (200 μm above apex) and CEZ (600 μm above apex). The data is presented as the ratio between the signal at the concave and the convex sides of the root. Error bars represent mean ± SE (3 biological independent experiments, n=20). No significant difference was found among different hydrostimulation times (Tukey-HSD post hoc-test ($P < 0.05$)).

Figure 2: Ascorbate accelerates root hydrotropic growth, and a mutant deficient in APX1 shows attenuated hydrotropic bending. A) Seedlings performing hydrotropic bending 2.5 h post hydrostimulation in the presence or absence of 1 mM sodium ascorbate. In both A and C) g represents gravity vector, Ψ represents water potential gradient, Scale bar, 1 mm. B) Root curvature kinetics and growth rate of ascorbate-treated hydrostimulated seedlings. Root curvature was measured at 1 h interval for 7 h following hydrostimulation. Root growth rate was determined by measuring the length at the beginning and at the end of the experiment. Error bars represent mean ± SE (3 biological independent experiments, 10 seedlings each). *p <0.05, Student's t-test for independent measurements. C) Root hydrotropic bending of WT and *apx1-2*, 5 h post hydrostimulation. D) Root curvature kinetics and growth rate of *apx1-2* and WT hydrostimulated seedlings. Root curvature and root growth rate were measured as described in B).

Figure 3: Application of DPI, an NADPH oxidase inhibitor, accelerates hydrotropism while delaying gravitropism. A) Application of 10 μM Diphenyleneiodonium (DPI) to the growing medium promotes hydrotropic curvature (first two left panels), and impedes gravitropic curvature (two right panels). Images were taken 2 h post hydrostimulation (scale bar, 1 mm) and 12 h post gravistimulation (scale bar, 5 mm). *g* represents gravity vector, Ψ represents water potential gradient. B) Root curvature was measured at 1 h interval for 6 h following hydrostimulation and at 2 h interval for 12 h following gravistimulation. Error bars represent mean ± SE (3 biological independent experiments, 10 seedlings each). C) DPI inhibits root growth in both physiological assays. Root growth rate was determined by measuring length at the beginning and at the end of the experiment. Error bars represent mean ± SE (3 biological independent experiments, 10 seedlings each). **p<0.01, t-test for independent measurements.

Figure 4: DPI eliminates ROS levels at the epidermal layer of the root elongation zone and elevates ROS levels at the meristematic zone. A, C and D) DHR fluorescence (in A, over bright field, in C and D, fluorescent channel only) of seedlings treated for 2 h with 10 μM DPI or DMSO for control. Scale bars, 100 μm in all confocal images. *g* represents gravity vector, Ψ represents water potential gradient. A) Images of unstimulated roots, pre-treated for 2 h with 10 μM DPI or DMSO. DHR signal is more intense and penetrates to the deeper root layers due to longer incubation in the dye (5 minutes). Images are representatives of n=23 seedlings. B) DHR

fluorescence intensity of seedlings treated with DPI or DMSO for 2 h, measured at the epidermal layer of the EZ and at the meristematic zone. Error bars represent mean ± SE (3 biological independent experiments, n=23 seedlings in total). *p<0.05, **p<0.01, t-test for independent measurements. C) Seedlings pre-treated with DPI for 2 h were gravistimulated, and show less ROS accumulation and asymmetrical distribution at the EZ. Images shown here are of a more extraneous section of the root, where the differences between DPI-treatment and control are highly detectable. Images are representatives of n = 11 seedlings. D) Seedlings that were hydrostimulated for 2 h on a DPI containing medium showing elimination of the signal from the epidermal layer at the bending region, which became more proximal to the root tip. Images are representatives of n = 20 seedlings.

Figure 5: *rbohC*, but not *rbohD*, show accelerated hydrotropic bending and lower ROS levels in the root apex. A) Root hydrotropic growth of WT, *rbohC* and *rbohD*, 2 h post hydrostimulation. Scale bar, 1 mm. g represents gravity vector, Ψ represents water potential gradient. B) Root curvature kinetics and growth rates. Root curvature was measured at 1 h interval for 7 hours following hydrostimulation. Root growth rate was determined by measuring length at the beginning and at the end of the experiment. Error bars represent mean ± SE (3 biological independent experiments, 10 seedlings each). Statistical difference in root curvature was tested for 2 and 5 h post hydrostimulation. C) Determination of H2O2 content in root apices (1-2 mm from tip) and whole seedlings (D) of WT, *rbohD* and *rbohC*, measured by the Amplex red assay (Materials and Methods). The fluorescent reads were normalized to the amount of extracted protein, measured by the Bradford assay. Error bars represent mean ± SD (3 biological repeats with two technical replicates. for root apices, n = 60, for whole seedlings, n = 20). The higher y-scale in C is a result of normalization to ten-fold lower protein level extracted from root apices. In B, C and D) Means with different letters are significantly different ($p < 0.05$, Tukey HSD adjusted comparisons).

Figure 6: Hydrotropism abrogates the gravitropic ROS signal. A) Schematic presentation of the assay applied to test ROS distribution at root tips of hydrostimulated seedlings and a combined gravistimulation with hydrostimulation. B) Roots were hydrostimulated for the indicated times and then gravistimulation for 1 h, stained with Dihydrorhodamin-123 (DHR) and imaged using a confocal microscope (Materials & Methods). Images are presented as pseudo color. Scale bar, 100 µm. C) Quantification of DHR fluorescence, measured at the DEZ epidermal layer (200 µm above apex). The data is presented as the ratio between the signal at the concave and the convex

565 sides of the root. Error bars represent mean ± SE (3 biological independent experiments, n=20).
566 D) Root curvature of 1 h gravistimulated seedlings following hydrostimulation for the indicated
567 times. The 1 h gravitropic curvature following 0, 2, 3 and 4 h hydrosimulation was 14.42° ±
568 1.27, 9.16° ± 0.76, 6.33° ± 0.78 and -3.14° ± 2.03, respectively. Error bars represent mean ± SE
569 (3 biological independent experiments, n=15). Negative value means curvature against the
570 gravity vector direction. In A and B, Ψ and g represent the water potential gradient and gravity
571 vector, respectively. ROS images of hydrostimulated roots for the same indicated times, without
572 gravistimulation are shown in Fig. 1 E. In C and D, letters above bars represent statistically
573 significant differences by Tukey-HSD post hoc-test ($P < 0.05$).

574

575 ## References

576 **Antoni R, Dietrich D, Bennett MJ, Rodriguez PL** (2016) Hydrotropism: Analysis of the Root
577 Response to a Moisture Gradient. Environ Responses Plants Methods Protoc 3–9

578 **Antoni R, Gonzalez-Guzman M, Rodriguez L, Peirats-Llobet M, Pizzio GA, Fernandez**
579 **MA, De Winne N, De Jaeger G, Dietrich D, Bennett MJ, et al** (2013) PYRABACTIN
580 RESISTANCE1-LIKE8 plays an important role for the regulation of abscisic acid signaling
581 in root. Plant Physiol **161**: 931–941

582 **Band LR, Wells DM, Larrieu A, Sun J, Middleton AM, French AP, Brunoud G, Sato EM,**
583 **Wilson MH, Péret B** (2012) Root gravitropism is regulated by a transient lateral auxin
584 gradient controlled by a tipping-point mechanism. Proc Natl Acad Sci **109**: 4668–4673

585 **Brady SM, Orlando DA, Lee J-Y, Wang JY, Koch J, Dinneny JR, Mace D, Ohler U, Benfey**
586 **PN** (2007) A high-resolution root spatiotemporal map reveals dominant expression patterns.
587 Science (80-) **318**: 801–806

588 **Brightman a O, Barr R, Crane FL, Morré DJ** (1988) Auxin-Stimulated NADH Oxidase
589 Purified from Plasma Membrane of Soybean. Plant Physiol **86**: 1264–9

590 **Brunoud G, Wells DM, Oliva M, Larrieu A, Mirabet V, Burrow AH, Beeckman T,**
591 **Kepinski S, Traas J, Bennett MJ** (2012) A novel sensor to map auxin response and
592 distribution at high spatio-temporal resolution. Nature **482**: 103–106

593 **Chen P, Umeda M** (2015) DNA double-strand breaks induce the expression of flavin-containing
594 monooxygenase and reduce root meristem size in *Arabidopsis thaliana*. Genes to Cells **20**:
595 636–646

596 **Cholodny NG** (1927) Wuchshormone und Tropismen bei den Pflanzen. Biol Zent 47:604-626.

597 **Crow JP** (1997) Dichlorodihydrofluorescein and dihydrorhodamine 123 are sensitive indicators
598 of peroxynitritein vitro: implications for intracellular measurement of reactive nitrogen and
599 oxygen species. Nitric oxide **1**: 145–157

600 **Darwin C, Darwin F** (1880) The power of movement in plants. John Murray

Davletova S, Rizhsky L, Liang H, Shengqiang Z, Oliver DJ, Coutu J, Shulaev V, Schlauch K, Mittler R (2005) Cytosolic ascorbate peroxidase 1 is a central component of the reactive oxygen gene network of Arabidopsis. Plant Cell **17**: 268–281

Douda DN, Khan MA, Grasemann H, Palaniyar N (2015) SK3 channel and mitochondrial ROS mediate NADPH oxidase-independent NETosis induced by calcium influx. Proc Natl Acad Sci **112**: 2817–2822

Dunand C, Crèvecoeur M, Penel C (2007) Distribution of superoxide and hydrogen peroxide in Arabidopsis root and their influence on root development: Possible interaction with peroxidases. New Phytol **174**: 332–341

Eapen D, Barroso ML, Ponce G, Campos ME, Cassab GI (2005) Hydrotropism: root growth responses to water. Trends Plant Sci **10**: 44–50

Fasano JM, Swanson SJ, Blancaflor EB, Dowd PE, Kao T, Gilroy S (2001) Changes in root cap pH are required for the gravity response of the Arabidopsis root. Plant Cell **13**: 907–921

Foreman J, Demidchik V, Bothwell JHF, Mylona P, Miedema H, Angel M, Linstead P, Costa S, Brownlee C, Jones JDG, et al (2003) Reactive oxygen species produced by NADPH oxidase regulate plant cell growth. Nature **422**: 442–446

Foyer CH, Noctor G (2005) Redox Homeostasis and Antioxidant Signaling: A Metabolic Interface between Stress Perception and Physiological Responses. Plant Cell Online **17**: 1866–1875

Friml J, Wiśniewska J, Benková E, Mendgen K, Palme K (2002) Lateral relocation of auxin efflux regulator PIN3 mediates tropism in Arabidopsis. Nature **415**: 806–809

Gomes A, Fernandes E, Lima JLFC (2005) Fluorescence probes used for detection of reactive oxygen species. J Biochem Biophys Methods **65**: 45–80

Hohl M, Greiner H, Schopfer P (1995) The cryptic-growth response of maize coleoptiles and its relationship to H2O2-dependent cell wall stiffening. Physiol Plant **94**: 491–498

Ivanchenko MG, Den Os D, Monshausen GB, Dubrovsky JG, Bednářová A, Krishnan N (2013) Auxin increases the hydrogen peroxide (H2O2) concentration in tomato (Solanum lycopersicum) root tips while inhibiting root growth. Ann Bot **112**: 1107–1116

Jaffe MJ, Takahashi H, Biro RL (1985) A pea mutant for the study of hydrotropism in roots. Science (80-) **230**: 445–447

Joo JH, Bae YS, Lee JS (2001) Role of Auxin-Induced Reactive Oxygen Species in Gravitropism. Plant Physiol **126**: 1055–1060

Joo JH, Yoo HJ, Hwang I, Lee JS, Nam KH, Bae YS (2005) Auxin-induced reactive oxygen species production requires the activation of phosphatidylinositol 3-kinase. FEBS Lett **579**: 1243–1248

Kaneyasu T, Kobayashi A, Nakayama M, Fujii N, Takahashi H, Miyazawa Y (2007) Auxin response, but not its polar transport, plays a role in hydrotropism of Arabidopsis roots. J Exp Bot **58**: 1143–1150

Kobayashi A, Takahashi A, Kakimoto Y, Miyazawa Y, Fujii N, Higashitani A, Takahashi H (2007) A gene essential for hydrotropism in roots. Proc Natl Acad Sci **104**: 4724–4729

Kögl F, Haagen-Smit AJ, Erxleben H (1934) Über ein neues Auxin („Hetero-auxin “) aus Harn. 11. Mitteilung über pflanzliche Wachstumsstoffe. Hoppe-Seyler´ s Zeitschrift für Physiol Chemie **228**: 90–103

Kwak JM, Mori IC, Pei ZM, Leonhardt N, Angel Torres M, Dangl JL, Bloom RE, Bodde S, Jones JDG, Schroeder JI (2003) NADPH oxidase *AtrbohD* and *AtrbohF* genes function in ROS-dependent ABA signaling in *Arabidopsis*. EMBO J **22**: 2623–2633

Massa GD, Gilroy S (2003) Touch modulates gravity sensing to regulate the growth of primary roots of Arabidopsis thaliana. Plant J **33**: 435–445

Miller EW, Dickinson BC, Chang CJ (2010) Aquaporin-3 mediates hydrogen peroxide uptake to regulate downstream intracellular signaling. Proc Natl Acad Sci **107**: 15681–15686

Miller G, Schlauch K, Tam R, Cortes D, Torres M a, Shulaev V, Dangl JL, Mittler R (2009) The plant NADPH oxidase RBOHD mediates rapid systemic signaling in response to diverse stimuli. Sci Signal **2**: ra45

Mittler R, Vanderauwera S, Suzuki N, Miller G, Tognetti VB, Vandepoele K, Gollery M, Shulaev V, Van Breusegem F (2011) ROS signaling: the new wave? Trends Plant Sci **16**: 300–309

Monshausen GB, Bibikova TN, Messerli M a, Shi C, Gilroy S (2007) Oscillations in extracellular pH and reactive oxygen species modulate tip growth of Arabidopsis root hairs. Proc Natl Acad Sci U S A **104**: 20996–1001

Monshausen GB, Bibikova TN, Weisenseel MH, Gilroy S (2009) Ca2+ regulates reactive oxygen species production and pH during mechanosensing in Arabidopsis roots. Plant Cell **21**: 2341–2356

Murashige T, Skoog F (1962) A revised medium for rapid growth and bio assays with tobacco tissue cultures. Physiol Plant **15**: 473–497

Nakayama M, Kaneko Y, Miyazawa Y, Fujii N, Higashitani N, Wada S, Ishida H, Yoshimoto K, Shirasu K, Yamada K, et al (2012) A possible involvement of autophagy in amyloplast degradation in columella cells during hydrotropic response of Arabidopsis roots. Planta **236**: 999–1012

Peer WA, Cheng Y, Murphy AS (2013) Evidence of oxidative attenuation of auxin signalling. J Exp Bot **64**: 2629–2639

Ponce G, Rasgado F, Cassab GI (2008) How amyloplasts, water deficit and root tropisms interact? Plant Signal Behav **3**: 460–462

Rashotte a M, Brady SR, Reed RC, Ante SJ, Muday GK (2000) Basipetal auxin transport is required for gravitropism in roots of Arabidopsis. Plant Physiol **122**: 481–490

Royall JA, Ischiropoulos H (1993) Evaluation of 2′, 7′-dichlorofluorescin and dihydrorhodamine 123 as fluorescent probes for intracellular H 2 O 2 in cultured endothelial cells. Arch Biochem Biophys **302**: 348–355

Von Sachs J (1887) Lecture XXVII. Relations between growth and cell-division in the embryonic tissues. Lect plant Physiol clarendon Press Oxford 431–459

Sagi M, Fluhr R (2006) Production of Reactive Oxygen Species by Plant NADPH oxidases. Plant Physiol **141**: 336–340

682 **Sarath G, Hou G, Baird LM, Mitchell RB** (2007) Reactive oxygen species, ABA and nitric
683 oxide interactions on the germination of warm-season C4-grasses. Planta **226**: 697–708

684 **Schippers JH, Foyer CH, van Dongen JT** (2016) Redox regulation in shoot growth, SAM
685 maintenance and flowering. Curr Opin Plant Biol **29**: 121–128

686 **Sharma SS, Dietz K-J** (2009) The relationship between metal toxicity and cellular redox
687 imbalance. Trends Plant Sci **14**: 43–50

688 **Shkolnik D, Krieger G, Nuriel R, Fromm H** (2016) Hydrotropism: root bending does not
689 require auxin redistribution. Mol Plant. doi: 10.1016/j.molp.2016.02.001

690 **Suzuki N, Miller G, Morales J, Shulaev V, Torres MA, Mittler R** (2011) Respiratory burst
691 oxidases: the engines of ROS signaling. Curr Opin Plant Biol **14**: 691–699

692 **Suzuki N, Miller G, Sejima H, Harper J, Mittler R** (2013) Enhanced seed production under
693 prolonged heat stress conditions in Arabidopsis thaliana plants deficient in cytosolic
694 ascorbate peroxidase 2. J Exp Bot **64**: 253–263

695 **Takahashi H, Miyazawa Y, Fujii N** (2009) Hormonal interactions during root tropic growth:
696 hydrotropism versus gravitropism. Plant Mol Biol **69**: 489–502

697 **Takahashi H, Suge H** (1991) Root hydrotropism of an agravitropic pea mutant, ageotropum.
698 Physiol Plant **82**: 24–31

699 **Takahashi N, Goto N, Okada K, Takahashi H** (2002) Hydrotropism in abscisic acid, wavy,
700 and gravitropic mutants of Arabidopsis thaliana. Planta **216**: 203–211

701 **Takahashi N, Yamazaki Y, Kobayashi A, Higashitani A, Takahashi H** (2003) Hydrotropism
702 Interacts with Gravitropism by Degrading Amyloplasts in Seedling Roots of Arabidopsis
703 and Radish. Plant Physiol **132**: 805–810

704 **Thimann K V** (1935) On the plant growth hormone produced by Rhizopus suinus. J Biol Chem
705 **109**: 279–291

706 **Tsukagoshi H, Busch W, Benfey PN** (2010) Transcriptional regulation of ROS controls
707 transition from proliferation to differentiation in the root. Cell **143**: 606–616

708 **Went FW** (1926) On growth-accelerating substances in the coleoptile of Avena sativa. Proc K
709 Ned Akad Wet. pp 10–19

710 **Winter D, Vinegar B, Nahal H, Ammar R, Wilson G V, Provart NJ** (2007) An "Electronic
711 Fluorescent Pictograph" browser for exploring and analyzing large-scale biological data
712 sets. PLoS One **2**: e718–e718

713 **Xu Y, Xu Q, Huang B** (2015) Ascorbic acid mitigation of water stress-inhibition of root growth
714 in association with oxidative defense in tall fescue (Festuca arundinacea Schreb.). Front
715 Plant Sci **6**: 1–14

716 **Young LM, Evans ML** (1994) Calcium-dependent asymmetric movement of 3H-indole-3-acetic
717 acid across gravistimulated isolated root caps of maize. Plant Growth Regul **14**: 235–242

718

719

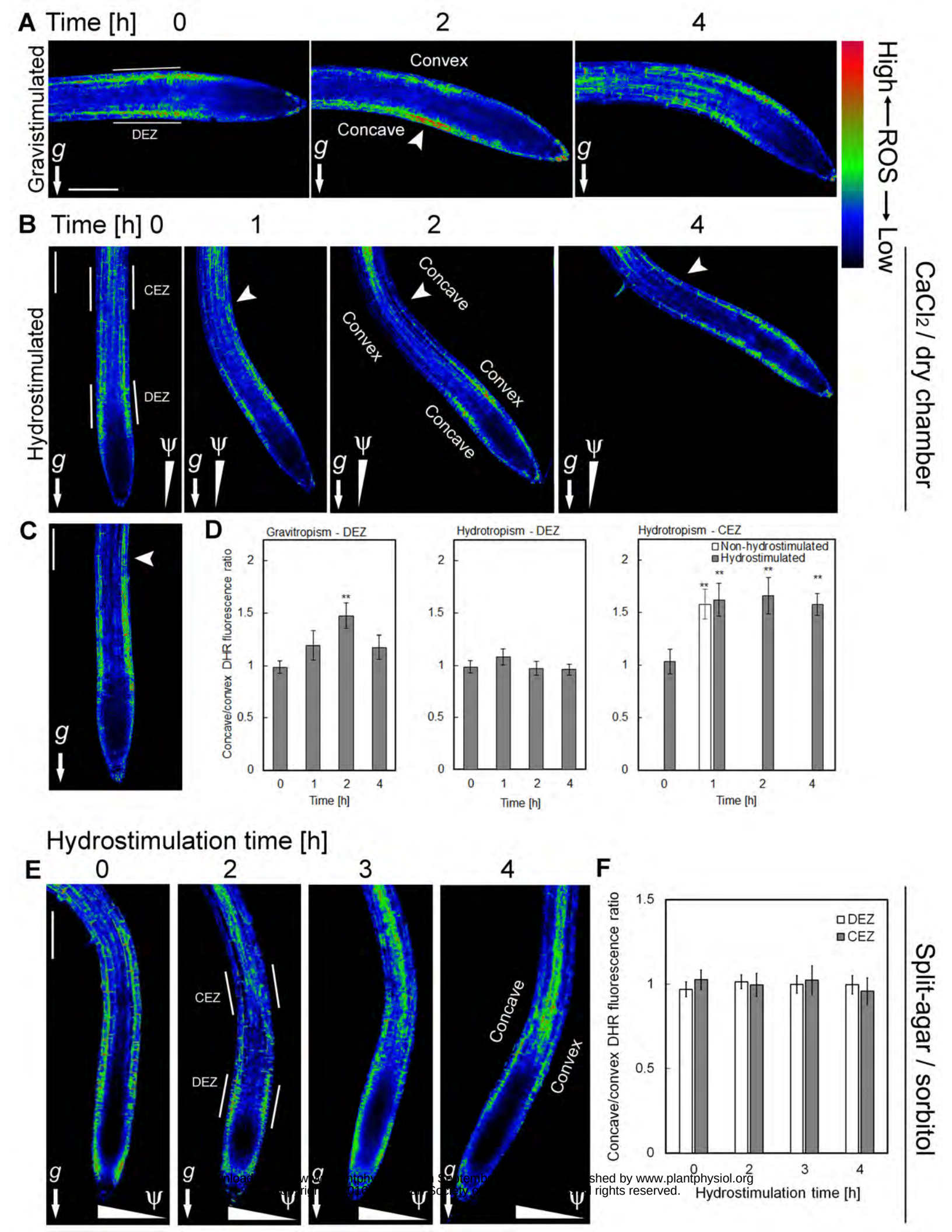

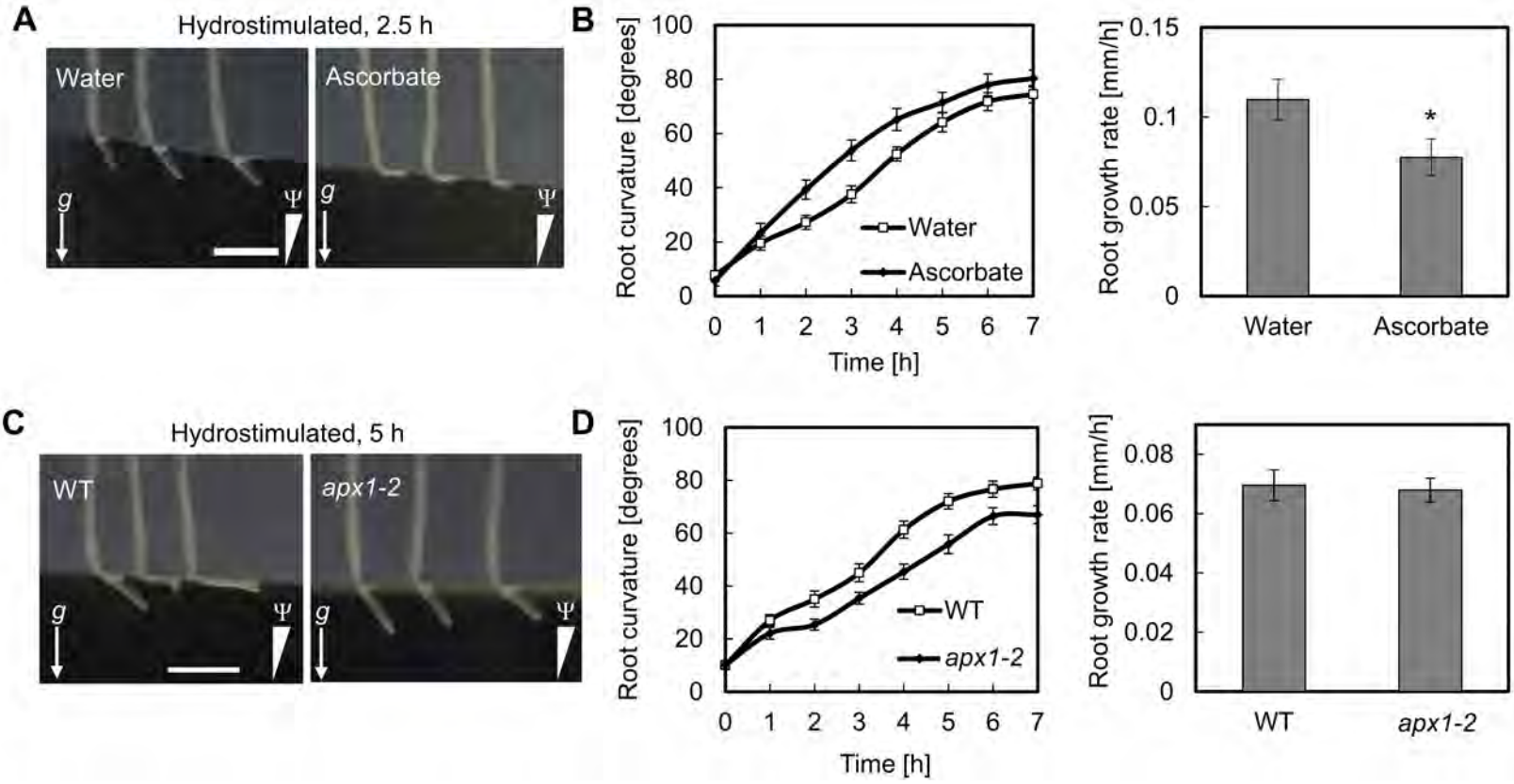

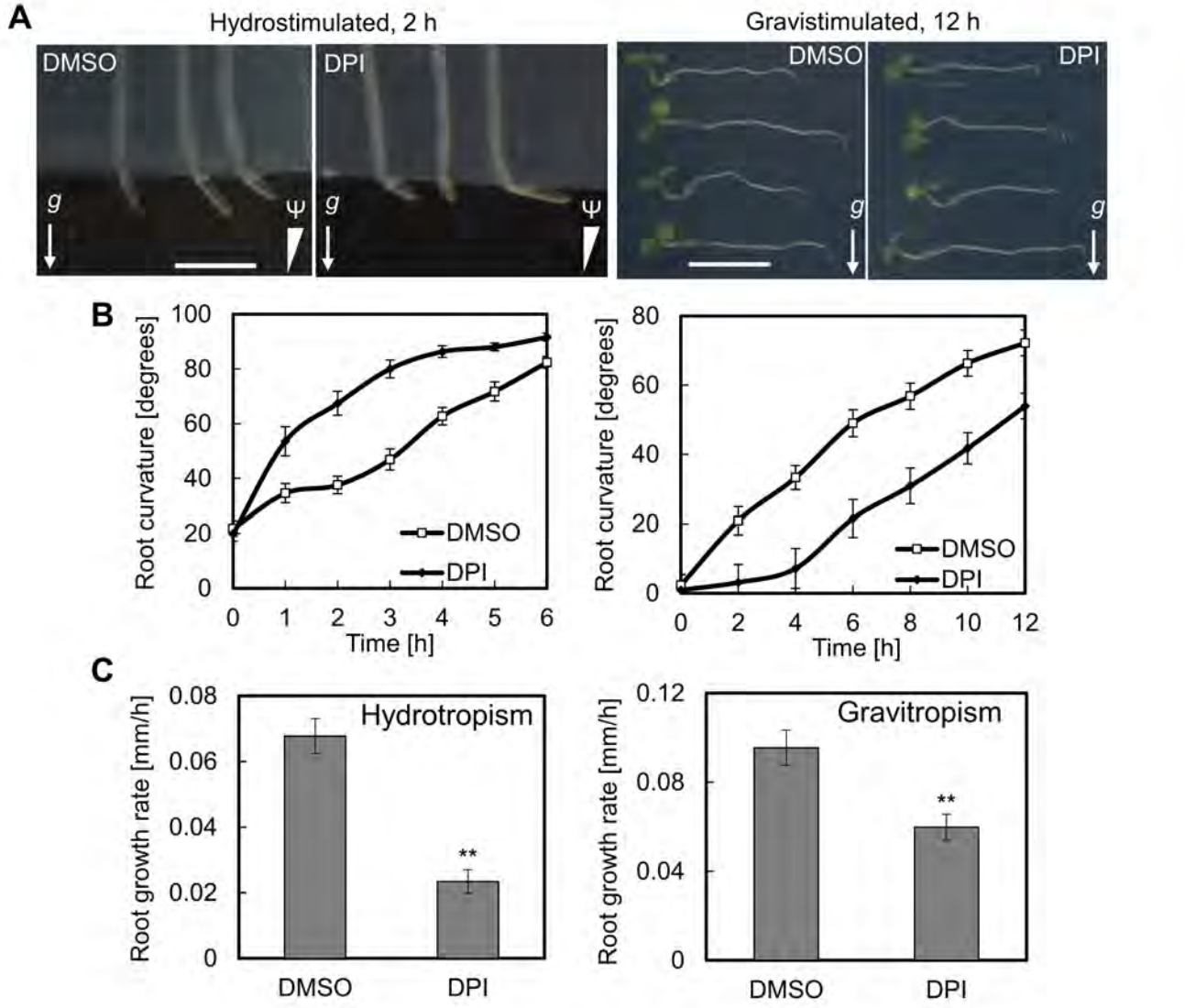

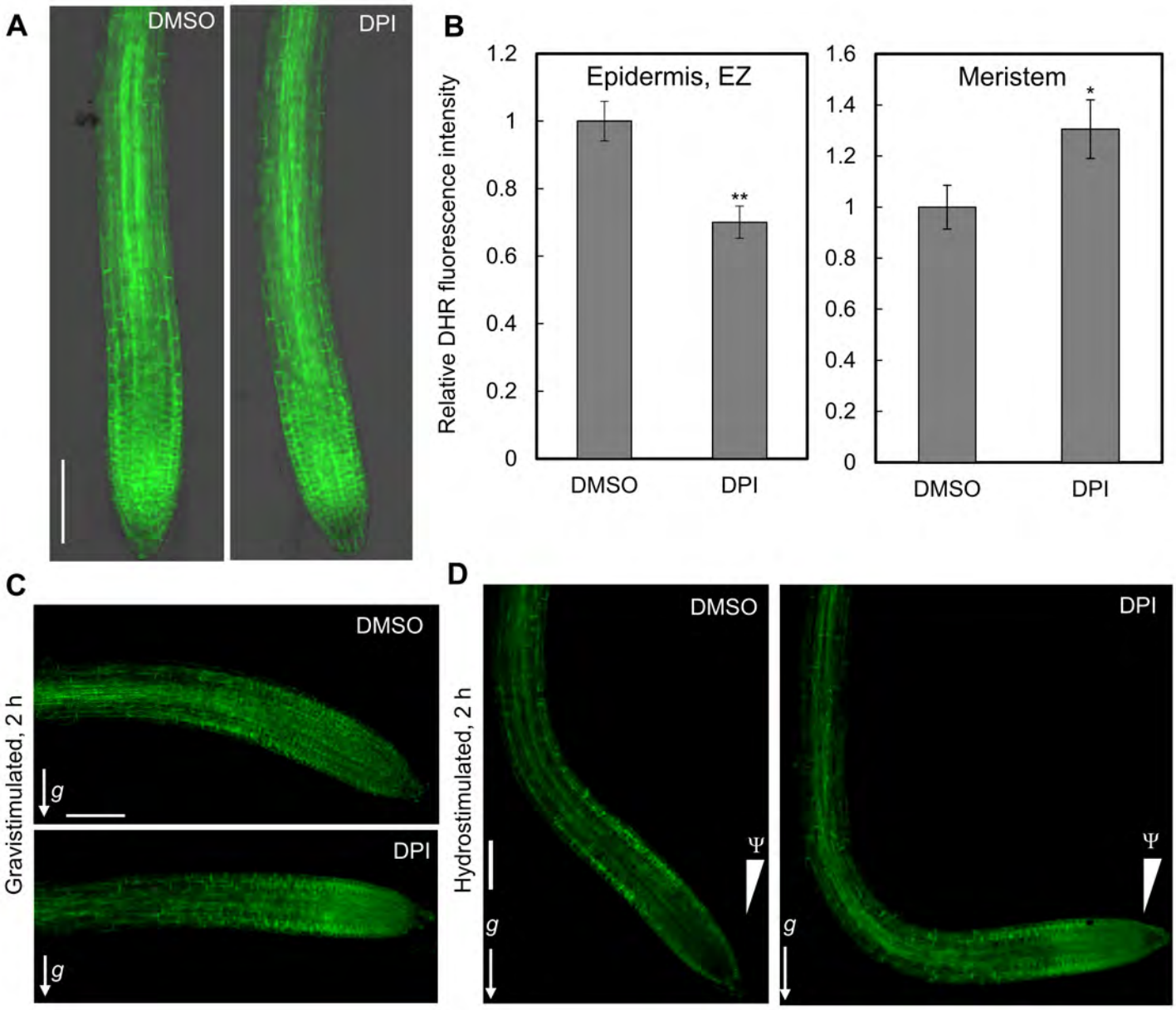

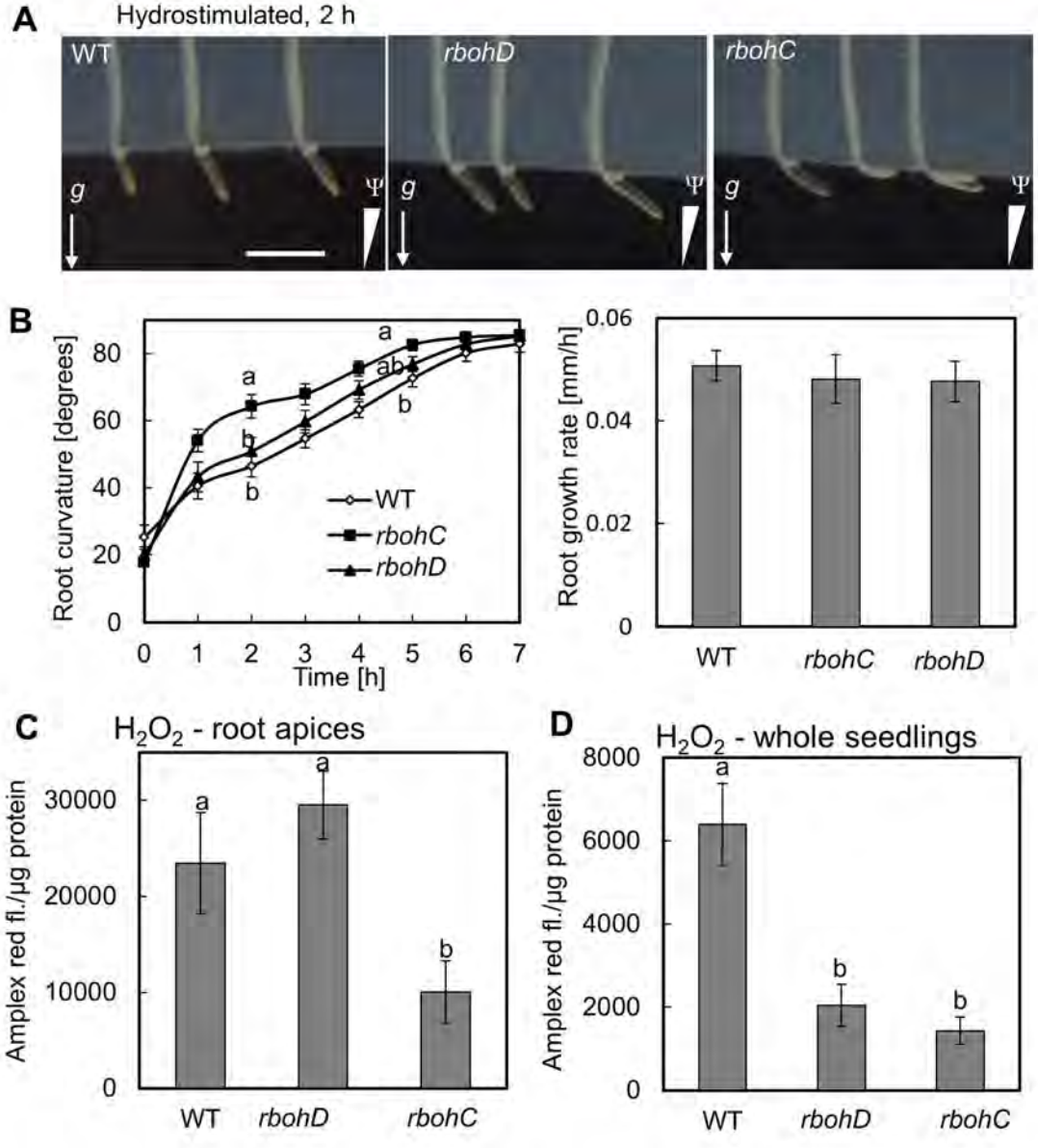

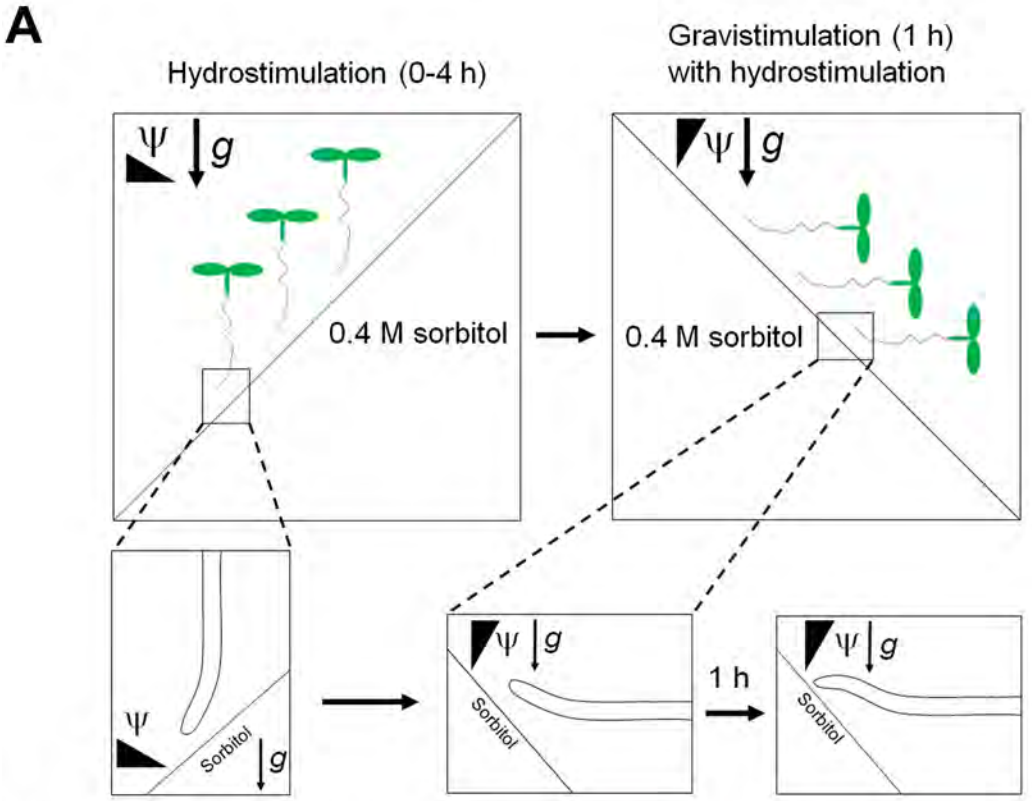

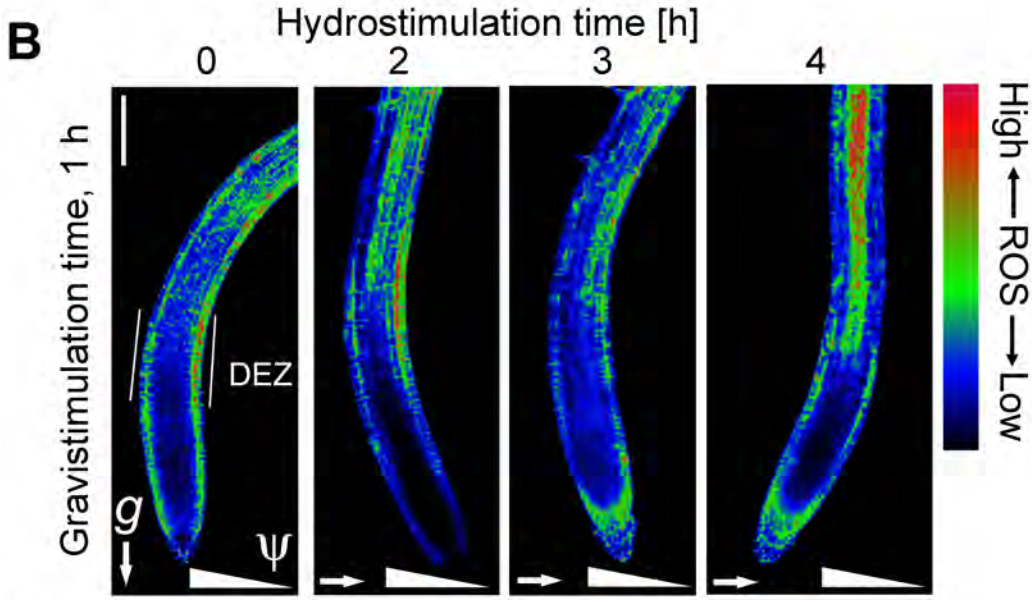

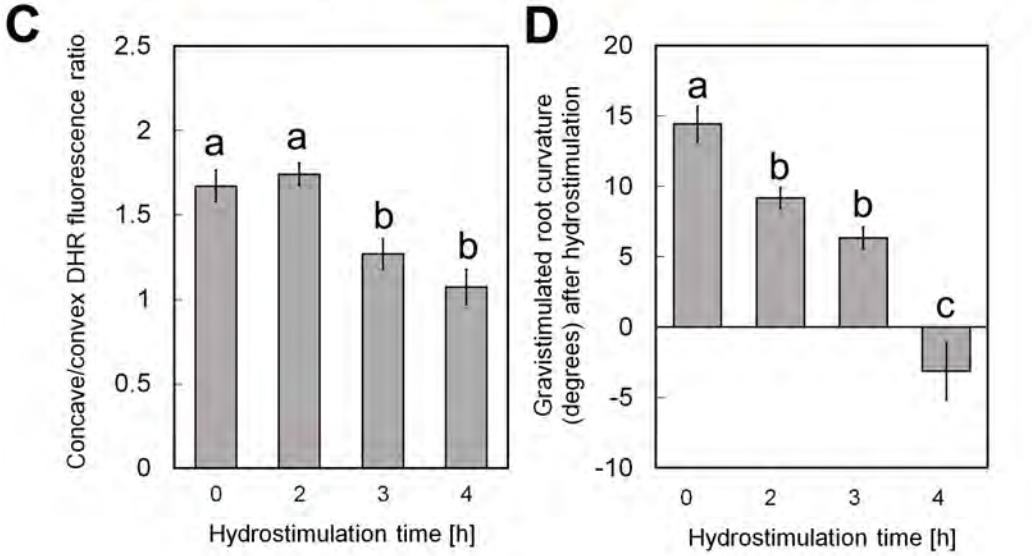

Parsed Citations

Antoni R, Dietrich D, Bennett MJ, Rodriguez PL (2016) Hydrotropism: Analysis of the Root Response to a Moisture Gradient. Environ Responses Plants Methods Protoc 3-9

Pubmed: Author and Title
CrossRef: Author and Title
Google Scholar: Author Only Title Only Author and Title

Antoni R, Gonzalez-Guzman M, Rodriguez L, Peirats-Llobet M, Pizzio GA, Fernandez MA, De Winne N, De Jaeger G, Dietrich D, Bennett MJ, et al (2013) PYRABACTIN RESISTANCE1-LIKE8 plays an important role for the regulation of abscisic acid signaling in root. Plant Physiol 161: 931-941

Pubmed: Author and Title
CrossRef: Author and Title
Google Scholar: Author Only Title Only Author and Title

Band LR, Wells DM, Larrieu A, Sun J, Middleton AM, French AP, Brunoud G, Sato EM, Wilson MH, Péret B (2012) Root gravitropism is regulated by a transient lateral auxin gradient controlled by a tipping-point mechanism. Proc Natl Acad Sci 109: 4668-4673

Pubmed: Author and Title
CrossRef: Author and Title
Google Scholar: Author Only Title Only Author and Title

Brady SM, Orlando DA, Lee J-Y, Wang JY, Koch J, Dinneny JR, Mace D, Ohler U, Benfey PN (2007) A high-resolution root spatiotemporal map reveals dominant expression patterns. Science (80-) 318: 801-806

Pubmed: Author and Title
CrossRef: Author and Title
Google Scholar: Author Only Title Only Author and Title

Brightman a O, Barr R, Crane FL, Morré DJ (1988) Auxin-Stimulated NADH Oxidase Purified from Plasma Membrane of Soybean. Plant Physiol 86: 1264-9

Pubmed: Author and Title
CrossRef: Author and Title
Google Scholar: Author Only Title Only Author and Title

Brunoud G, Wells DM, Oliva M, Larrieu A, Mirabet V, Burrow AH, Beeckman T, Kepinski S, Traas J, Bennett MJ (2012) A novel sensor to map auxin response and distribution at high spatio-temporal resolution. Nature 482: 103-106

Pubmed: Author and Title
CrossRef: Author and Title
Google Scholar: Author Only Title Only Author and Title

Chen P, Umeda M (2015) DNA double-strand breaks induce the expression of flavin-containing monooxygenase and reduce root meristem size in Arabidopsis thaliana. Genes to Cells 20: 636-646

Pubmed: Author and Title
CrossRef: Author and Title
Google Scholar: Author Only Title Only Author and Title

Cholodny NG (1927) Wuchshormone und Tropismen bei den Pflanzen. Biol Zent 47:604-626.

Pubmed: Author and Title
CrossRef: Author and Title
Google Scholar: Author Only Title Only Author and Title

Crow JP (1997) Dichlorodihydrofluorescein and dihydrorhodamine 123 are sensitive indicators of peroxynitritein vitro: implications for intracellular measurement of reactive nitrogen and oxygen species. Nitric oxide 1: 145-157

Pubmed: Author and Title
CrossRef: Author and Title
Google Scholar: Author Only Title Only Author and Title

Darwin C, Darwin F (1880) The power of movement in plants. John Murray

Pubmed: Author and Title
CrossRef: Author and Title
Google Scholar: Author Only Title Only Author and Title

Davletova S, Rizhsky L, Liang H, Shengqiang Z, Oliver DJ, Coutu J, Shulaev V, Schlauch K, Mittler R (2005) Cytosolic ascorbate peroxidase 1 is a central component of the reactive oxygen gene network of Arabidopsis. Plant Cell 17: 268-281

Pubmed: Author and Title
CrossRef: Author and Title
Google Scholar: Author Only Title Only Author and Title

Douda DN, Khan MA, Grasemann H, Palaniyar N (2015) SK3 channel and mitochondrial ROS mediate NADPH oxidase-independent NETosis induced by calcium influx. Proc Natl Acad Sci 112: 2817-2822

Pubmed: Author and Title
CrossRef: Author and Title
Google Scholar: Author Only Title Only Author and Title

Dunand C, Crèvecoeur M, Penel C (2007) Distribution of superoxide and hydrogen peroxide in Arabidopsis root and their influence on root development: Possible interaction with peroxidases. New Phytol 174: 332-341

Pubmed: Author and Title
CrossRef: Author and Title
Google Scholar: Author Only Title Only Author and Title

Eapen D, Barroso ML, Ponce G, Campos ME, Cassab GI (2005) Hydrotropism: root growth responses to water. Trends Plant Sci 10:

44-50
Pubmed: Author and Title
CrossRef: Author and Title
Google Scholar: Author Only Title Only Author and Title

Fasano JM, Swanson SJ, Blancaflor EB, Dowd PE, Kao T, Gilroy S (2001) Changes in root cap pH are required for the gravity response of the Arabidopsis root. Plant Cell 13: 907-921
Pubmed: Author and Title
CrossRef: Author and Title
Google Scholar: Author Only Title Only Author and Title

Foreman J, Demidchik V, Bothwell JHF, Mylona P, Miedema H, Angel M, Linstead P, Costa S, Brownlee C, Jones JDG, et al (2003) Reactive oxygen species produced by NADPH oxidase regulate plant cell growth. Nature 422: 442-446
Pubmed: Author and Title
CrossRef: Author and Title
Google Scholar: Author Only Title Only Author and Title

Foyer CH, Noctor G (2005) Redox Homeostasis and Antioxidant Signaling: A Metabolic Interface between Stress Perception and Physiological Responses. Plant Cell Online 17: 1866-1875
Pubmed: Author and Title
CrossRef: Author and Title
Google Scholar: Author Only Title Only Author and Title

Friml J, Wisniewska J, Benková E, Mendgen K, Palme K (2002) Lateral relocation of auxin efflux regulator PIN3 mediates tropism in Arabidopsis. Nature 415: 806-809
Pubmed: Author and Title
CrossRef: Author and Title
Google Scholar: Author Only Title Only Author and Title

Gomes A, Fernandes E, Lima JLFC (2005) Fluorescence probes used for detection of reactive oxygen species. J Biochem Biophys Methods 65: 45-80
Pubmed: Author and Title
CrossRef: Author and Title
Google Scholar: Author Only Title Only Author and Title

Hohl M, Greiner H, Schopfer P (1995) The cryptic-growth response of maize coleoptiles and its relationship to H2O2-dependent cell wall stiffening. Physiol Plant 94: 491-498
Pubmed: Author and Title
CrossRef: Author and Title
Google Scholar: Author Only Title Only Author and Title

Ivanchenko MG, Den Os D, Monshausen GB, Dubrovsky JG, Bednárová A, Krishnan N (2013) Auxin increases the hydrogen peroxide (H2O2) concentration in tomato (Solanum lycopersicum) root tips while inhibiting root growth. Ann Bot 112: 1107-1116
Pubmed: Author and Title
CrossRef: Author and Title
Google Scholar: Author Only Title Only Author and Title

Jaffe MJ, Takahashi H, Biro RL (1985) A pea mutant for the study of hydrotropism in roots. Science (80-) 230: 445-447
Pubmed: Author and Title
CrossRef: Author and Title
Google Scholar: Author Only Title Only Author and Title

Joo JH, Bae YS, Lee JS (2001) Role of Auxin-Induced Reactive Oxygen Species in Gravitropism. Plant Physiol 126: 1055-1060
Pubmed: Author and Title
CrossRef: Author and Title
Google Scholar: Author Only Title Only Author and Title

Joo JH, Yoo HJ, Hwang I, Lee JS, Nam KH, Bae YS (2005) Auxin-induced reactive oxygen species production requires the activation of phosphatidylinositol 3-kinase. FEBS Lett 579: 1243-1248
Pubmed: Author and Title
CrossRef: Author and Title
Google Scholar: Author Only Title Only Author and Title

Kaneyasu T, Kobayashi A, Nakayama M, Fujii N, Takahashi H, Miyazawa Y (2007) Auxin response, but not its polar transport, plays a role in hydrotropism of Arabidopsis roots. J Exp Bot 58: 1143-1150
Pubmed: Author and Title
CrossRef: Author and Title
Google Scholar: Author Only Title Only Author and Title

Kobayashi A, Takahashi A, Kakimoto Y, Miyazawa Y, Fujii N, Higashitani A, Takahashi H (2007) A gene essential for hydrotropism in roots. Proc Natl Acad Sci 104: 4724-4729
Pubmed: Author and Title
CrossRef: Author and Title
Google Scholar: Author Only Title Only Author and Title

Kögl F, Haagen-Smit AJ, Erxleben H (1934) Über ein neues Auxin („Hetero-auxin ") aus Harn. 11. Mitteilung über pflanzliche Wachstumsstoffe. Hoppe-Seyler´ s Zeitschrift für Physiol Chemie 228: 90-103
Pubmed: Author and Title
CrossRef: Author and Title
Google Scholar: Author Only Title Only Author and Title

Kwak JM, Mori IC, Pei ZM, Leonhardt N, Angel Torres M, Dangl JL, Bloom RE, Bodde S, Jones JDG, Schroeder JI (2003) NADPH oxidase AtrbohD and AtrbohF genes function in ROS-dependent ABA signaling in Arabidopsis. EMBO J 22: 2623-2633
Pubmed: Author and Title
CrossRef: Author and Title
Google Scholar: Author Only Title Only Author and Title

Massa GD, Gilroy S (2003) Touch modulates gravity sensing to regulate the growth of primary roots of Arabidopsis thaliana. Plant J 33: 435-445
Pubmed: Author and Title
CrossRef: Author and Title
Google Scholar: Author Only Title Only Author and Title

Miller EW, Dickinson BC, Chang CJ (2010) Aquaporin-3 mediates hydrogen peroxide uptake to regulate downstream intracellular signaling. Proc Natl Acad Sci 107: 15681-15686
Pubmed: Author and Title
CrossRef: Author and Title
Google Scholar: Author Only Title Only Author and Title

Miller G, Schlauch K, Tam R, Cortes D, Torres M a, Shulaev V, Dangl JL, Mittler R (2009) The plant NADPH oxidase RBOHD mediates rapid systemic signaling in response to diverse stimuli. Sci Signal 2: ra45
Pubmed: Author and Title
CrossRef: Author and Title
Google Scholar: Author Only Title Only Author and Title

Mittler R, Vanderauwera S, Suzuki N, Miller G, Tognetti VB, Vandepoele K, Gollery M, Shulaev V, Van Breusegem F (2011) ROS signaling: the new wave? Trends Plant Sci 16: 300-309
Pubmed: Author and Title
CrossRef: Author and Title
Google Scholar: Author Only Title Only Author and Title

Monshausen GB, Bibikova TN, Messerli M a, Shi C, Gilroy S (2007) Oscillations in extracellular pH and reactive oxygen species modulate tip growth of Arabidopsis root hairs. Proc Natl Acad Sci U S A 104: 20996-1001
Pubmed: Author and Title
CrossRef: Author and Title
Google Scholar: Author Only Title Only Author and Title

Monshausen GB, Bibikova TN, Weisenseel MH, Gilroy S (2009) Ca2+ regulates reactive oxygen species production and pH during mechanosensing in Arabidopsis roots. Plant Cell 21: 2341-2356
Pubmed: Author and Title
CrossRef: Author and Title
Google Scholar: Author Only Title Only Author and Title

Murashige T, Skoog F (1962) A revised medium for rapid growth and bio assays with tobacco tissue cultures. Physiol Plant 15: 473-497
Pubmed: Author and Title
CrossRef: Author and Title
Google Scholar: Author Only Title Only Author and Title

Nakayama M, Kaneko Y, Miyazawa Y, Fujii N, Higashitani N, Wada S, Ishida H, Yoshimoto K, Shirasu K, Yamada K, et al (2012) A possible involvement of autophagy in amyloplast degradation in columella cells during hydrotropic response of Arabidopsis roots. Planta 236: 999-1012
Pubmed: Author and Title
CrossRef: Author and Title
Google Scholar: Author Only Title Only Author and Title

Peer WA, Cheng Y, Murphy AS (2013) Evidence of oxidative attenuation of auxin signalling. J Exp Bot 64: 2629-2639
Pubmed: Author and Title
CrossRef: Author and Title
Google Scholar: Author Only Title Only Author and Title

Ponce G, Rasgado F, Cassab GI (2008) How amyloplasts, water deficit and root tropisms interact? Plant Signal Behav 3: 460-462
Pubmed: Author and Title
CrossRef: Author and Title
Google Scholar: Author Only Title Only Author and Title

Rashotte a M, Brady SR, Reed RC, Ante SJ, Muday GK (2000) Basipetal auxin transport is required for gravitropism in roots of Arabidopsis. Plant Physiol 122: 481-490
Pubmed: Author and Title
CrossRef: Author and Title
Google Scholar: Author Only Title Only Author and Title

Royall JA, Ischiropoulos H (1993) Evaluation of 2', 7'-dichlorofluorescin and dihydrorhodamine 123 as fluorescent probes for intracellular H 2 O 2 in cultured endothelial cells. Arch Biochem Biophys 302: 348-355
Pubmed: Author and Title
CrossRef: Author and Title
Google Scholar: Author Only Title Only Author and Title

Von Sachs J (1887) Lecture XXVII. Relations between growth and cell-division in the embryonic tissues. Lect plant Physiol clarendon Press Oxford 431-459
Pubmed: Author and Title

CrossRef: Author and Title
Google Scholar: Author Only Title Only Author and Title

Sagi M, Fluhr R (2006) Production of Reactive Oxygen Species by Plant NADPH oxidases. Plant Physiol 141: 336-340
Pubmed: Author and Title
CrossRef: Author and Title
Google Scholar: Author Only Title Only Author and Title

Sarath G, Hou G, Baird LM, Mitchell RB (2007) Reactive oxygen species, ABA and nitric oxide interactions on the germination of warm-season C4-grasses. Planta 226: 697-708
Pubmed: Author and Title
CrossRef: Author and Title
Google Scholar: Author Only Title Only Author and Title

Schippers JH, Foyer CH, van Dongen JT (2016) Redox regulation in shoot growth, SAM maintenance and flowering. Curr Opin Plant Biol 29: 121-128
Pubmed: Author and Title
CrossRef: Author and Title
Google Scholar: Author Only Title Only Author and Title

Sharma SS, Dietz K-J (2009) The relationship between metal toxicity and cellular redox imbalance. Trends Plant Sci 14: 43-50
Pubmed: Author and Title
CrossRef: Author and Title
Google Scholar: Author Only Title Only Author and Title

Shkolnik D, Krieger G, Nuriel R, Fromm H (2016) Hydrotropism: root bending does not require auxin redistribution. Mol Plant. doi: 10.1016/j.molp.2016.02.001
Pubmed: Author and Title
CrossRef: Author and Title
Google Scholar: Author Only Title Only Author and Title

Suzuki N, Miller G, Morales J, Shulaev V, Torres MA, Mittler R (2011) Respiratory burst oxidases: the engines of ROS signaling. Curr Opin Plant Biol 14: 691-699
Pubmed: Author and Title
CrossRef: Author and Title
Google Scholar: Author Only Title Only Author and Title

Suzuki N, Miller G, Sejima H, Harper J, Mittler R (2013) Enhanced seed production under prolonged heat stress conditions in Arabidopsis thaliana plants deficient in cytosolic ascorbate peroxidase 2. J Exp Bot 64: 253-263
Pubmed: Author and Title
CrossRef: Author and Title
Google Scholar: Author Only Title Only Author and Title

Takahashi H, Miyazawa Y, Fujii N (2009) Hormonal interactions during root tropic growth: hydrotropism versus gravitropism. Plant Mol Biol 69: 489-502
Pubmed: Author and Title
CrossRef: Author and Title
Google Scholar: Author Only Title Only Author and Title

Takahashi H, Suge H (1991) Root hydrotropism of an agravitropic pea mutant, ageotropum. Physiol Plant 82: 24-31
Pubmed: Author and Title
CrossRef: Author and Title
Google Scholar: Author Only Title Only Author and Title

Takahashi N, Goto N, Okada K, Takahashi H (2002) Hydrotropism in abscisic acid, wavy, and gravitropic mutants of Arabidopsis thaliana. Planta 216: 203-211
Pubmed: Author and Title
CrossRef: Author and Title
Google Scholar: Author Only Title Only Author and Title

Takahashi N, Yamazaki Y, Kobayashi A, Higashitani A, Takahashi H (2003) Hydrotropism Interacts with Gravitropism by Degrading Amyloplasts in Seedling Roots of Arabidopsis and Radish. Plant Physiol 132: 805-810
Pubmed: Author and Title
CrossRef: Author and Title
Google Scholar: Author Only Title Only Author and Title

Thimann K V (1935) On the plant growth hormone produced by Rhizopus suinus. J Biol Chem 109: 279-291
Pubmed: Author and Title
CrossRef: Author and Title
Google Scholar: Author Only Title Only Author and Title

Tsukagoshi H, Busch W, Benfey PN (2010) Transcriptional regulation of ROS controls transition from proliferation to differentiation in the root. Cell 143: 606-616
Pubmed: Author and Title
CrossRef: Author and Title
Google Scholar: Author Only Title Only Author and Title

Went FW (1926) On growth-accelerating substances in the coleoptile of Avena sativa. Proc K Ned Akad Wet. pp 10-19
Pubmed: Author and Title
CrossRef: Author and Title
Google Scholar: Author Only Title Only Author and Title

Winter D, Vinegar B, Nahal H, Ammar R, Wilson G V, Provart NJ (2007) An "Electronic Fluorescent Pictograph" browser for exploring and analyzing large-scale biological data sets. PLoS One 2: e718-e718
Pubmed: Author and Title
CrossRef: Author and Title
Google Scholar: Author Only Title Only Author and Title

Xu Y, Xu Q, Huang B (2015) Ascorbic acid mitigation of water stress-inhibition of root growth in association with oxidative defense in tall fescue (Festuca arundinacea Schreb.). Front Plant Sci 6: 1-14
Pubmed: Author and Title
CrossRef: Author and Title
Google Scholar: Author Only Title Only Author and Title

Young LM, Evans ML (1994) Calcium-dependent asymmetric movement of 3H-indole-3-acetic acid across gravistimulated isolated root caps of maize. Plant Growth Regul 14: 235-242
Pubmed: Author and Title
CrossRef: Author and Title
Google Scholar: Author Only Title Only Author and Title

Supplemental Figures

Supplemental Figure S1

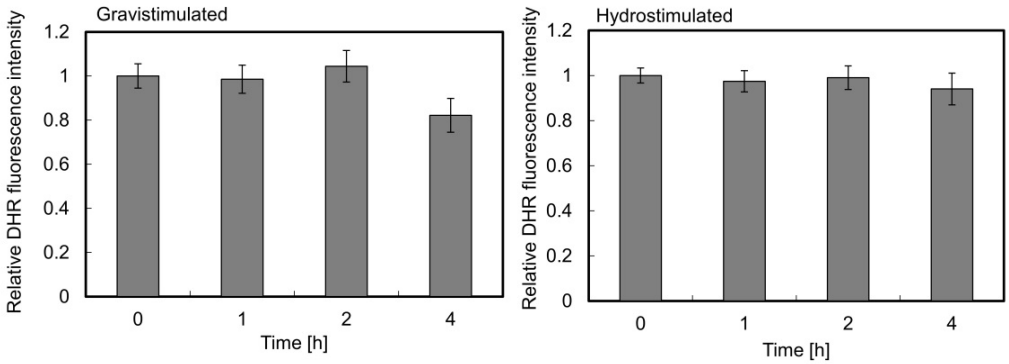

Supplemental Figure S1: Relative DHR fluorescence intensity in gravistimulated and hydrostimulated roots ($CaCl_2$ / dry chamber), measured at the indicated time points. Root were stained and imaged as in Fig. 1. Fluorescence intensity was measured in epidermis cells of root tip in a 700 µm segment above apex. Presented here is the fold change in fluorescence intensity from time 0. In each experimental system, t-test of each time point versus time 0 resulted in no significant difference.

Supplemental Figure S2

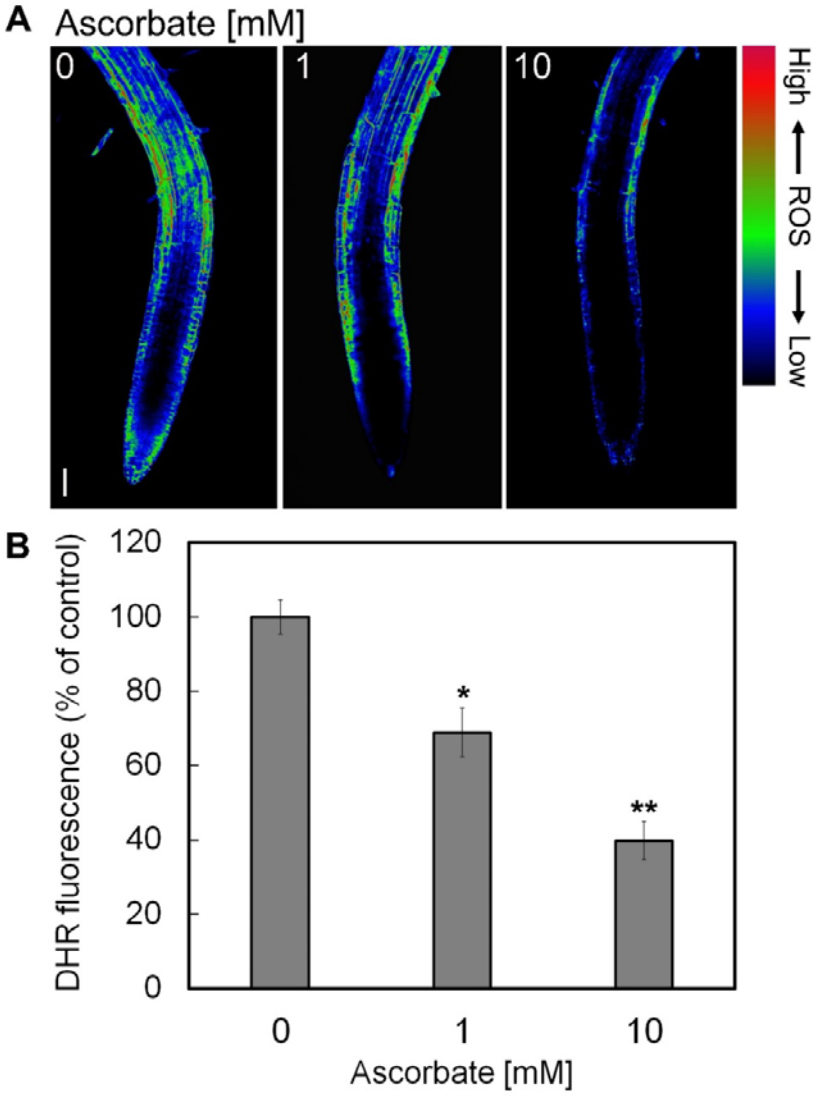

Supplemental Figure S2: ROS level is reduced by ascorbate. A) Five-day-old seedlings were placed on 1 mm Whatman filter paper soaked with 0.25 X MS supplemented with the indicated concentrations of ascorbate. DHR staining was performed after 1 h of treatment and fluorescence was visualized using confocal microscopy. Images are presented as pseudo-color. Scale bar, 50 µm. B) Quantification of DHR fluorescence measured in epidermal layer (longitudinal section image as in A, 700 µm from apex shootward). Error bars represent mean ± SE (3 biological independent experiments, 10 seedlings each). * P=0.0012, ** P=8.5×10^{-8} (student's t test) when comparing each treatment to control.

Supplemental Figure S3

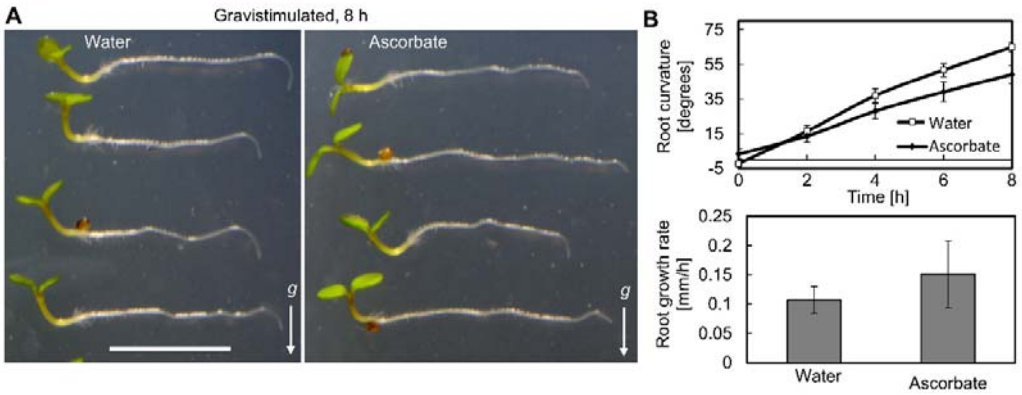

Supplemental Figure S3: The antioxidant ascorbate impedes root gravitropic response. A) Seedlings performing gravitropic bending 8 h post gravistimulation in the presence or absence of 1 mM sodium ascorbate. Scale bar, 5 mm, *g* represents gravity vector. B) Root curvature kinetics and growth rate of ascorbate treated gravistimulated seedlings. Root curvature was measured at 2 h intervals for 8 h following plate reorientation. Root growth rate was determined by measuring length at the beginning and at the end of the experiment. Error bars represent mean ± SE (3 biological independent experiments, 10 seedlings each).

Supplemental Figure S4

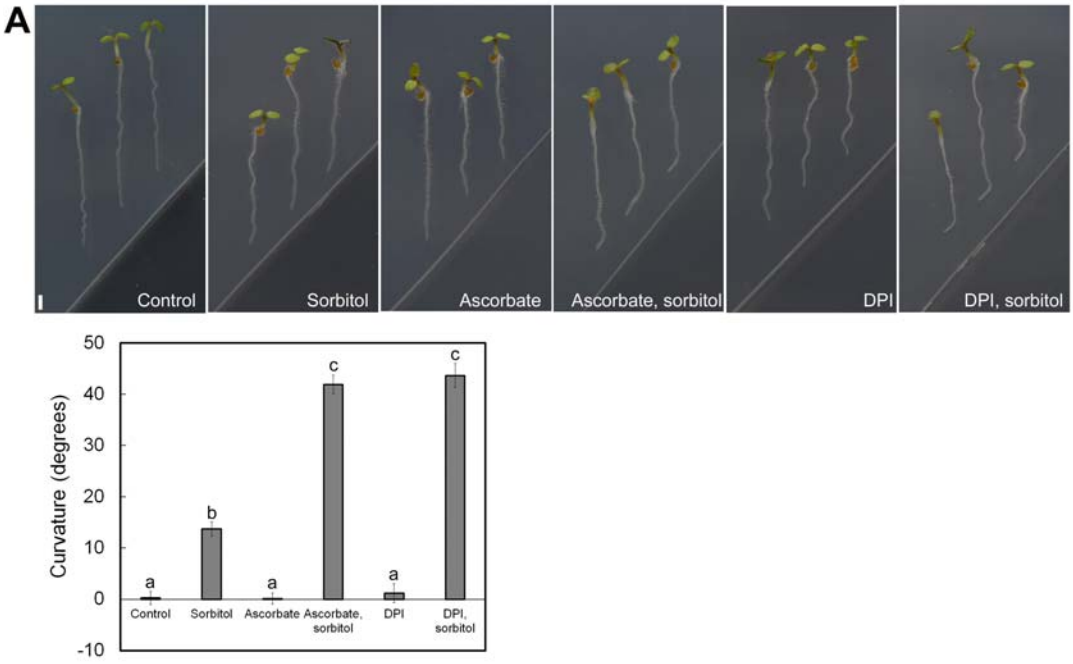

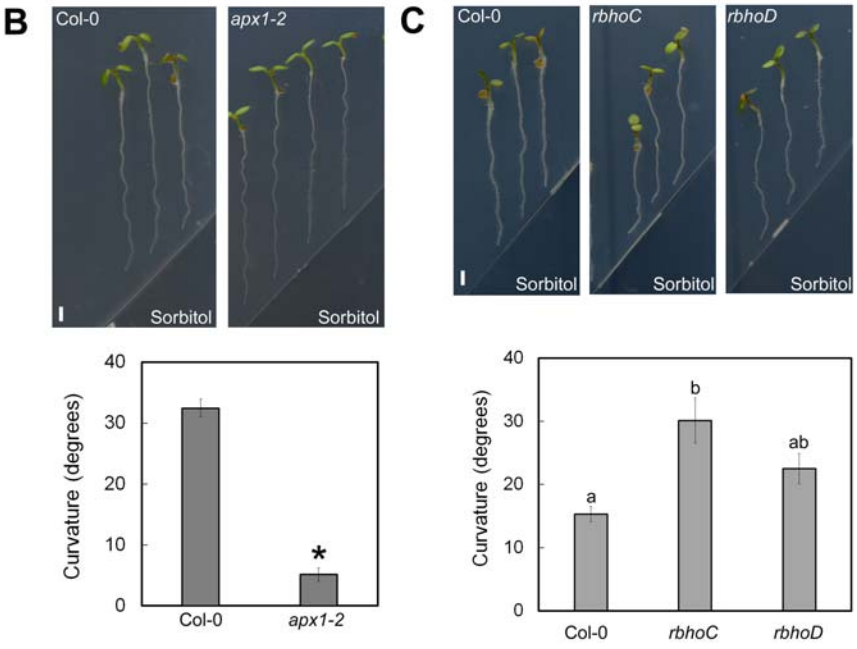

Supplemental Figure S4: Hydrostimulation using the split-agar / sorbitol method. A) Five-day-old WT seedlings were hydrostimulated with or without 2 mM ascorbate or 20 µM DPI in the sorbitol gel slice. Images were taken 6 h after treatment started. B) Seven-day-old WT and *apx1-2* seedlings were hydrostimulated for 8 h. C) Five-day-old WT, *rbhoC* and *rbhoD* seedlings were hydrostimulated for 6 h. In A, B and C, root tip curvature was measured in relevant images. Error bars represent mean ± SE (3 biological independent experiments, n=20). In A and C, letters above bars represent statically different values by Tukey-HSD post hoc-test ($P < 0.05$). In B, * $P < 0.05$ (student's *t* test).

Supplemental Figure S5

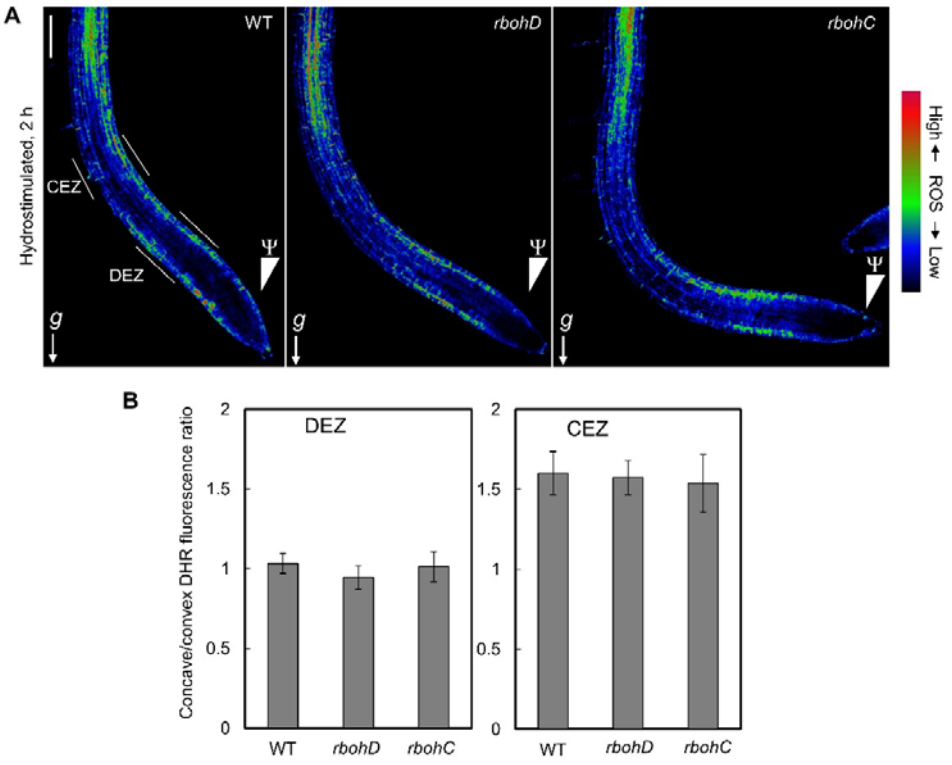

Supplemental Figure S5: ROS distribution during hydrotropic growth in WT, *rbohC* and *rbohD* mutants. A) Pseudo-colored confocal images of 2 h hydrostimulated roots of the indicated genotypes. *g* represents gravity vector, Ψ represents water potential gradient. Scale bar, 100 µm. B) Quantification of DHR fluorescence, measured at the epidermal layer in two regions of the root EZ. The data is presented as the ratio between the signal at the concave and the convex sides of the root. Error bars represent mean ± SE (3 biological independent experiments, n=28 for the DEZ, n = 18 for the CEZ). The differences in the ratio levels between genotypes, in each region are insignificant (ANOVA, 95% significance level).

Supplemental Figure S6

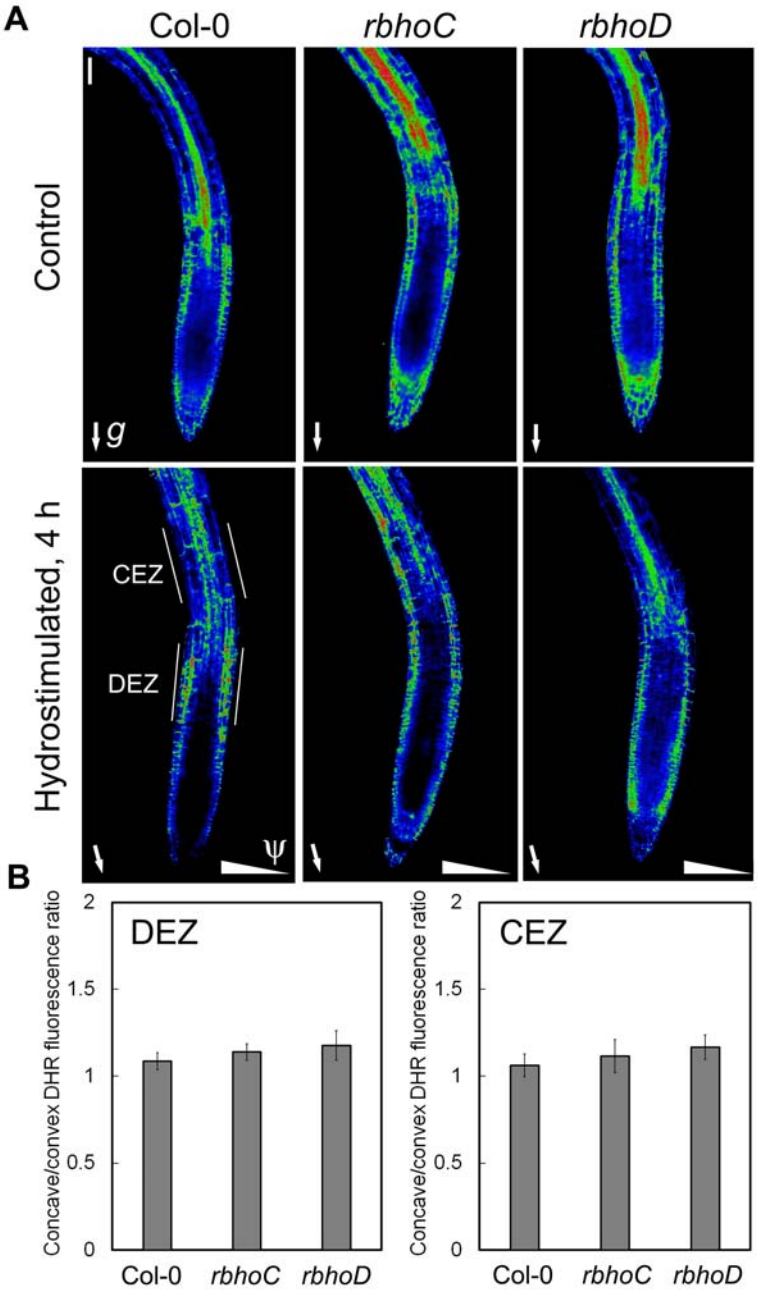

Supplemental Figure S6: ROS distribution in hydrostimulated WT, *rbohC* and *rbohD* mutants using the split-agar / sorbitol system. A) Five-day-old seedlings were hydrostimulated for 4 h prior to DHR staining and imaging. *g* represents gravity vector, Ψ represents water potential gradient. Scale bar, 50 µm. B) Quantification of DHR fluorescence, measured at the epidermal layer in two regions of the root EZ. The data is presented as the ratio between the signal at the concave and the convex sides of the root. Error bars represent mean ± SE (3 biological independent experiments, n=30 for the DEZ, n = 30 for the CEZ). The differences in the ratio levels between genotypes, in each region are insignificant (ANOVA, 95% significance level).

Supplemental Figure S7

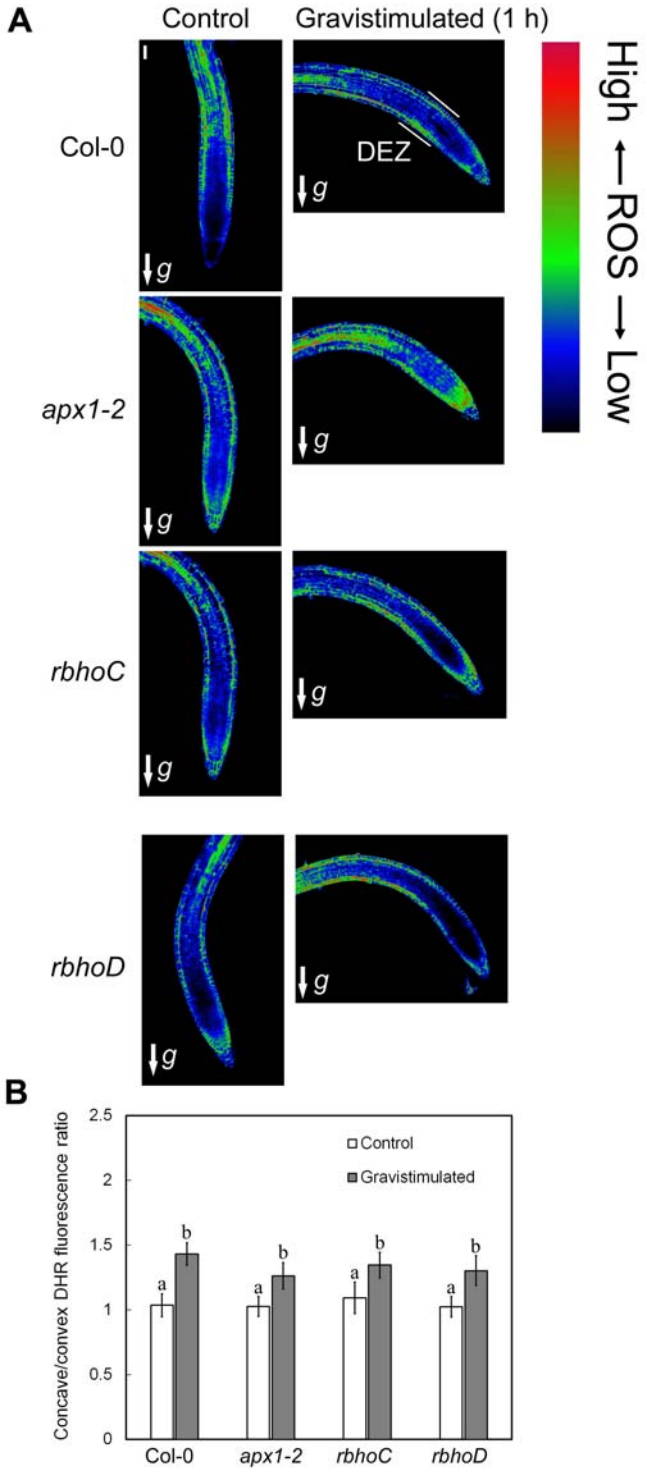

Supplemental Figure S7: ROS distribution in gravistimulated WT, *apx1-2*, *rbhoC* and *rbhoD* mutants. A) Control and 1 h gravistimulated roots of 5-day-old seedlings were stained with Dihydrorhodamine-123 (DHR) and imaged using confocal microscopy. Images are presented as pseudo color. Scale bar, 50 μm. B) Quantification of DHR fluorescence, measured at the EZ epidermal layer (200 μm above apex). The data is presented as the ratio between the signal at the concave and the convex sides of the root. Error bars represent mean ± SE (3 biological independent experiments, n=20). Letters above bars represent statically different values by Tukey-HSD post hoc-test ($P < 0.05$).

Supplemental Figure S8

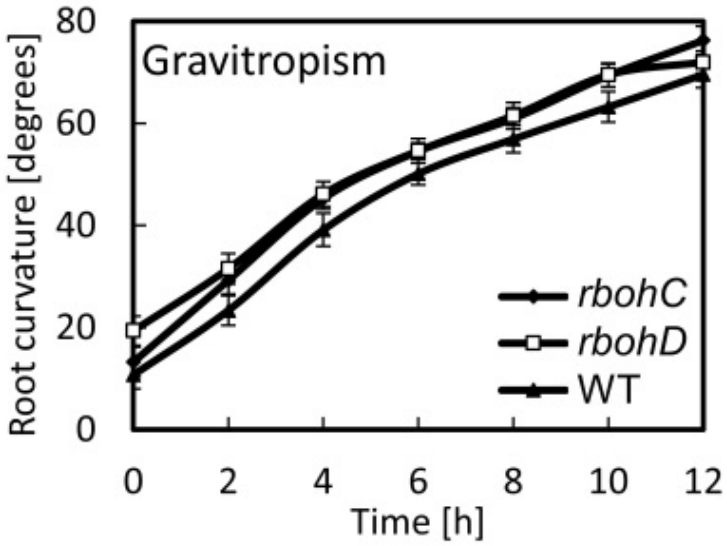

Supplemental Figure S8: *rbohC* and *rbohD* exhibit normal gravitropic growth compared to WT. Error bars represent mean ± SE (3 biological independent experiments, n=10 seedlings each).

Supplemental Figure S9

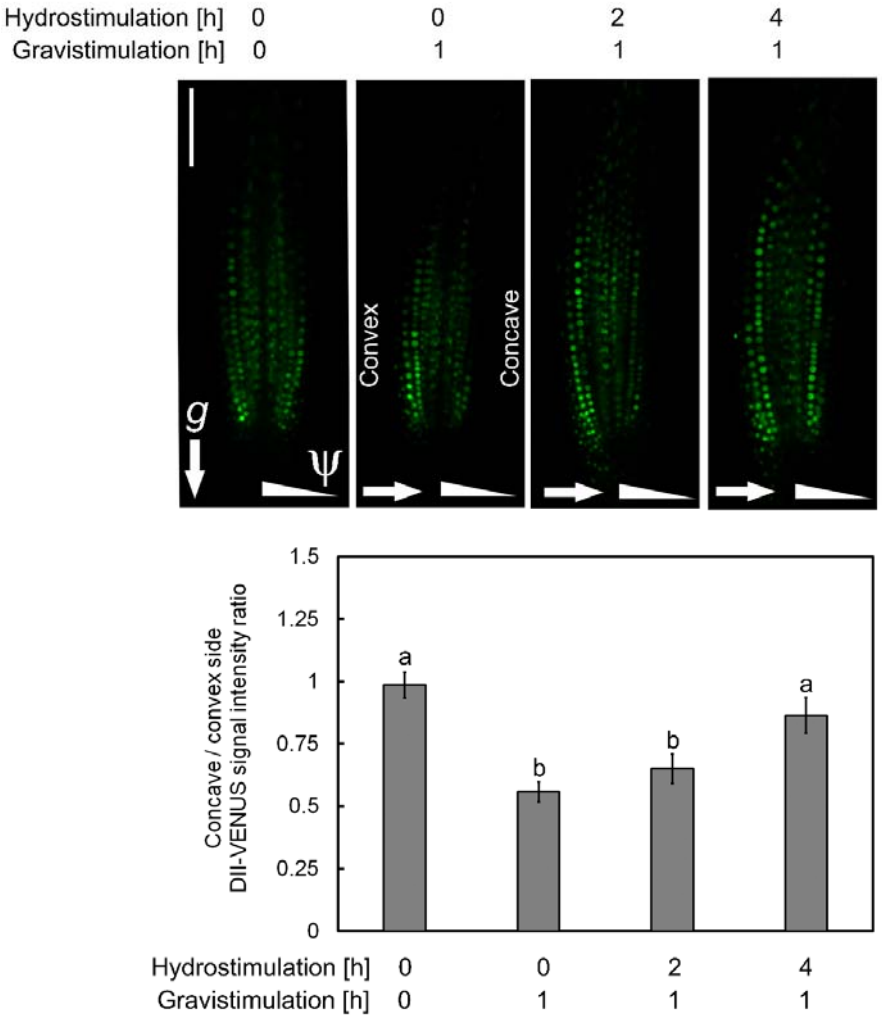

Supplemental Figure S9: Auxin distribution in gravistimulated root tips with or without prior hydrostimulation. A) DII-VENUS fluorescence was visualized by confocal microscopy in stimulated roots for the indicated times as previously described (Shkolnik et al., 2016). Scale bar, 100 µm. Arrows represent the direction of the gravity vector (*g*), and triangles depict the moisture gradient (ψ).

B) Quantification of the DII-VENUS signal intensity of stimulated root tips, measured at the epidermis and cortex tissues layers of both root sides, 40-240 µm above the root apex. The data is presented as the ratio between the fluorescent signal at the concave and the convex sides of the root tip. Error bars represent mean ± SE (2 biological independent experiments, n=15 seedlings each). Letters above bars represent statistically significant differences by the Tukey-HSD post hoc-test ($P < 0.05$).

Supplemental movies

Supplemental movies: Hydrotropism of *rbohC* (movie 1) and *rbohD* (movie 2) mutants compared to WT over a time period of seven hours. Time points are presented at the lower right corner. Photos were taken as described in Materials and Methods.